Manuscript revised for *Journal of Zoological Systematics and Evolutionary Research*

Multilocus phylogeny and species delimitation within the genus *Glauconycteris* (Chiroptera, Vespertilionidae), with the description of a new bat species from the Tshopo Province of the Democratic Republic of the Congo.

Alexandre Hassanin[1,2], Raphaël Colombo[3], Guy-Crispin Gembu[4], Marie Merle[1], Vuong Tan Tu[1,5], Tamás Görföl[6], Prescott Musaba Akawa[4], Gábor Csorba[6], Teresa Kearney[7,8], Ara Monadjem[9,10], Ros Kiri Ing[11]

[1] Institut de Systématique, Evolution, Biodiversité, Sorbonne Universités, Univ Paris 06, MNHN, CNRS; Muséum national d'Histoire naturelle, 55 rue Buffon, 75005 Paris, France.

[2] Muséum national d'Histoire naturelle, UMS 2700, 75005 Paris, France.

[3] Asellia Ecologie, 60 chemin de la Nuirie, 04200 Sisteron, France.

[4] Université de Kisangani, Faculté des Sciences, BP 2012 Kisangani, République Démocratique du Congo.

[5] Institute of Ecology and Biological Resources, Vietnam Academy of Science and Technology, 18, Hoang Quoc Viet road, Cau Giay district, Hanoi, Vietnam.

[6] Hungarian Natural History Museum, 1088 Budapest, Baross u. 13, Hungary.

[7] Ditsong National Museum of Natural History, PO Box 413, Pretoria, 0001, South Africa.

[8] School of Animal, Plant and Environmental Sciences, University of the Witwatersrand, Private Bag 3, Wits 2050, South Africa.

[9] Department of Biological Sciences, University of Swaziland, Private Bag 4, Kwaluseni, Swaziland.

[10] Mammal Research Institute, Department of Zoology & Entomology, University of Pretoria, Private Bag 20, Hatfield 0028, Pretoria, South Africa.

[11] Institut Langevin, UMR 7587 CNRS, Université Paris Diderot (Paris 7), Paris, France.

* Corresponding author; E-mail: hassanin@mnhn.fr; Tel: +33 1 40 79 56 93

ABSTRACT

The genus *Glauconycteris* Dobson, 1875 currently contains 12 species of butterfly bats, all endemic to sub-Saharan Africa. Most species are rarely recorded, with half of the species known from less than six geographic localities. The taxonomic status of several species remains problematic.

Here, we studied the systematics of butterfly bats using both morphological and molecular approaches. We examined 45 adult specimens for external anatomy and skull morphology, and investigated the phylogeny of *Glauconycteris* using DNA sequences from three mitochondrial genes and 116 individuals, which in addition to outgroup taxa, included nine of the twelve butterfly bat species currently recognized. Four additional nuclear genes were sequenced on a reduced sample of 69 individuals, covering the outgroup and *Glauconycteris* species. Our molecular results show that the genus *Glauconycteris* is monophyletic, and that it is the sister-group of the Asian genus *Hesperoptenus*. Molecular dating estimates based on either *Cytb* or *RAG2* data sets suggest that the ancestor of *Glauconycteris* migrated into Africa from Asia during the Tortonian age of the Late Miocene (11.6-7.2 Mya), while the basal diversification of the crown group occurred in Africa at around 6 ± 2 Mya. The species *G. superba* is found to be the sister-group of *G. variegata*, questioning its placement in the recently described genus *Niumbaha*. The small species living in tropical rainforests constitute a robust clade, which contains three divergent lineages: (i) the '*poensis*' group, which is composed of *G. poensis*, *G. alboguttata*, *G. argentata* and *G. egeria*; (ii) the '*beatrix*' group, which contains *G. beatrix* and *G. curryae*; and (iii) the '*humeralis*' group, which includes *G. humeralis* and a new species described herein. In the '*poensis*' group, *G. egeria* is found to be monophyletic in the nuclear tree, but polyphyletic in the mitochondrial tree. The reasons for this mito-nuclear discordance are discussed.

KEYWORDS: DNA phylogeny – taxonomy – morphology – new species – Africa – evergreen forest.

INTRODUCTION

The genus *Glauconycteris* Dobson, 1875 currently contains 12 species, which are all endemic to sub-Saharan Africa (ACR 2016; IUCN 2016; **Figure 1**). Their vernacular name, butterfly bats, apparently refers to some resemblance with a large butterfly or moth while in flight, as well as their attractive appearance (Happold and Happold 2013; Rambaldini 2010). The pelage of the pied butterfly bat (*Glauconycteris superba* Hayman, 1939) is probably the most spectacular, with a black body strikingly marked with white spots on the head and shoulders, and white stripes on the throat, along each side of the belly, and on the back. Most species are rarely recorded and poorly known: *Glauconycteris curryae* Eger and Schlitter, 2001; *Glauconycteris egeria* Thomas, 1913; *Glauconycteris gleni* Peterson and Smith, 1973; and *G. superba* have been collected from only a few localities (respectively 6, 6, 2, and 6); whereas *Glauconycteris machadoi* Hayman, 1963 and *Glauconycteris kenyacola* Peterson, 1982 are known only from the holotype (Happold and Happold 2013; ACR 2016; Ing et al. 2016).

In early classifications, *Glauconycteris* was treated as a subgenus of *Chalinolobus* (e.g. Dobson 1875; Ryan 1966; Koopman 1971; Koopman 1994), because the external appearance of butterfly bats was regarded as similar to that of the wattled and pied bats found in Oceania. However, based on skull and baculum differences, many authors have considered *Glauconycteris* and *Chalinolobus* as distinct genera (e.g. Miller 1907; Tate 1942; Hill and Harrison 1987; Happold and Happold 2013; ACR 2016). Molecular studies have shown that *Glauconycteris* and *Chalinolobus* are not closely related within the family Vespertilionidae (Hoofer and Van Den Bussche 2003; Roehrs et al. 2011; Koubínová et al. 2013). On the one hand, *Chalinolobus* was found to be closely related to *Nyctophilus* and *Vespadelus* (two other genera of Oceania) into a larger clade containing four additional genera *Hypsugo*, *Laephotis*, *Neoromicia*, and *Nycticeinops*. On the other hand, *Glauconycteris* was related to the genera *Arielulus*, *Eptesicus* (including *Histiotus macrotus*), *Hesperoptenus*, *Ia*, *Lasionycteris*, *Nycticeius*, and *Scotomanes*. However, the monophyly of this group (sometimes referred to as the tribe Nycticeiini) was poorly

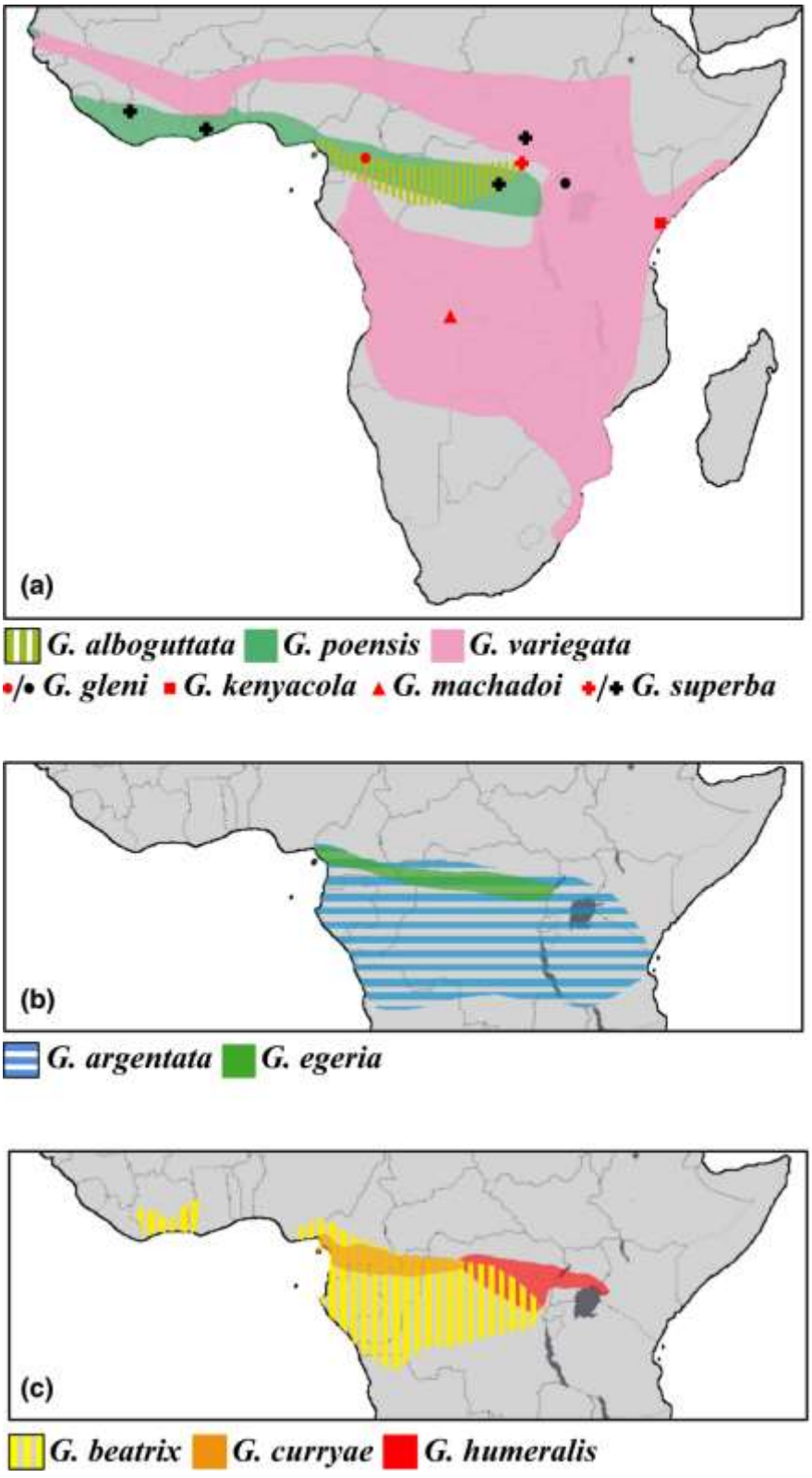

Figure 1. Geographic distributions of the 12 species currently recognized in the genus *Glauconycteris*.

The geographic ranges were modified from the maps provided by the IUCN (2016). The symbols (circle, square, triangle, cross) were used to indicate all localities (type locality in red) known for the four rarely collected species *G. gleni*, *G. kenyacola*, *G. machadoi* and *G. superba.* Note that the geographic ranges of *G. alboguttata*, *G. curryae*, and *G. egeria* may have been underestimated, as only a few specimens have been collected for these species.

supported and the position of *Glauconycteris* remained unresolved. Although only four species of *Glauconycteris* were represented in previous molecular studies, the genus was found to be monophyletic in the trees of Hoofer and Van Den Bussche (2003) and Roehrs et al. (2011), but *Arielulus cuprosus* was nested within *Glauconycteris* in the tree of Koubínová et al. (2013). Because of its unique morphology, the pied butterfly bat (*G. superba*) has been considered as the sister group of *Glauconycteris* sensu stricto and placed into its own genus *Niumbaha* by Reeder et al. (2013). This taxonomic hypothesis, however, has not been tested using molecular data.

Here, we carry out an integrated systematic study to clarify the taxonomic status of butterfly bats collected in 2013 in the Bas-Uele and Tshopo Provinces of the Democratic Republic of the Congo and in southern Central African Republic. A selection of 45 adult specimens is studied for external anatomy and skull morphology. The molecular phylogeny of the genus *Glauconycteris* is examined based on a data set including three mitochondrial and four nuclear genes (representing 6,179 characters), a diversity of outgroup taxa, and all species of *Glauconycteris*, except *G. gleni* and the two species known only from their holotype, *G. kenyacola* and *G. machadoi*. Our objectives were to address the following questions: (1) Is the genus *Glauconycteris* monophyletic? (2) Which genera are closely related to *Glauconycteris*? (3) What are the species relationships within *Glauconycteris*? (4) How did *Glauconycteris* evolve in geological time, specifically during the Neogene and Quaternary, with a particular interest in the biogeographic history and changes in coloration pattern?

MATERIALS AND METHODS

Taxonomic sampling

Most of the specimens analysed in this study were collected by some of the authors (AH, GCG, PMA, RC, TG, and VTT) using mist-nets (Ecotone, Gdynia, Poland) during field surveys conducted in the Bas-Uele and Tshopo Provinces of the Democratic Republic of the Congo (DRC) (samples identified in **Table S1** by the code "K13") and in the Lobaye and Sangha-

Mbaéré Provinces of the Central African Republic (CAR) (identified in **Table S1** by the codes "R08" and "R13", respectively). After capture, all bats were measured, photographed, and tentatively identified using the keys published in Rambaldini (2010) and Patterson and Webala (2012). For voucher specimens deposited in the MNHN collections (see details in **Table S1**), taxonomic identifications were refined after skull extraction using the data published in Allen (1917), Eger and Schlitter (2001), Happold and Happold (2013), Rosevear (1965), and Thomas (1901, 1913).

A few other specimens or samples were loaned by the following institutions: Ditsong National Museum of Natural History (formerly known as the Transvaal Museum; DNMNH; Pretoria, South Africa), Durban Natural Science Museum (DNSM; Durban, South Africa), Field museum of Natural History (FMNH; Chicago, USA), Hungarian Natural History Museum (HNHM; Budapest, Hungary), Iziko Museum (also known as the South African Museum [SAM]; Cape Town, South Africa), and Royal Ontario Museum (ROM; Toronto, Canada) (see details in **Table S1**).

Morphological analysis

A total of 45 adult specimens of *Glauconycteris* were examined for morphologically (**Tables S1 and S2**). Besides mass (W, expressed in grams), the following external measurements were taken using digital callipers accurate to 0.01 mm (acronym for each measurement presented in parentheses): forearm length (FA) – from the elbow to the wrist with both joints folded; head and body length (HB) – from the tip of the face to the anus; tail length (Tail) – from the anus to tip of the tail; tibia length (TIB) – from the knee to the ankle; the length of the 1st finger (F1); the lengths of 2nd, 3rd, 4th and 5th metacarpals (2DM, 3DM, 4DM and 5DM, respectively) – from the wrist to the end of the respective metacarpals; the lengths of the first and second phalanges of the 3rd digit (3D1P and 3D2P). After skull extraction, nine cranial and six dental measurements were taken using digital callipers accurate to 0.01 mm. Abbreviations and definitions for craniodental

measurements include: mandible length (ML) – greatest length of the mandible, measured from the front of incisors to the condylar processes; mandible width (MW) – width across outer points of right and left rami of the mandible; greatest length of skull (GLS) – from anterior-most point of teeth to the most posteriorly projecting point of the occipital region; zygomatic width (ZW) – greatest width of the skull across the zygomatic arches; braincase width (BCW) – greatest width of the braincase; braincase height (BCH) – from the base of the auditory bullae to the highest part of the skull; interorbital width (IOW) – least width of the interorbital constriction; mastoid breadth (MB) – greatest distance across skull at mastoid processes; least width of the palate (LWP); complete upper canine-molar toothrow (C-M^3), length from anterior alveolar border of upper canine (C^1) to posterior alveolar border of 3rd molar (M^3); width across upper canines (C^1-C^1), taken across the outer alveolar borders of the canines; width across 3rd upper molars (M^3-M^3), taken across the outer borders of the 3rd molars; complete lower canine-molar toothrow (C-M_3), length from anterior alveolar border of lower canine (C_1) to posterior alveolar border of 3rd molar (M_3); width across lower canines (C_1-C_1), taken across the outer alveolar borders of the canines; width across 3rd lower molars (M_3-M_3), taken across the outer borders of the 3rd molars.

Based on our observations, we also described the following 11 categorical variables: wing colour (WC), with four character-states (A: brown; B: pale; C: black; D: pale yellowish-orange with dark brown pigment); dorsal general colour (DGC), with seven character-states (A: blackish brown; B: grey / golden fawn; C: reddish brown; D: curry/reddish fawn; E: brown; F: piebald pattern; G: yellow); dorsal hairs (DH), with three character-states (A: unicolour; B: bicolour; C: tricolour); ventral general colour (VGC), with three character-states (A: lighter than dorsal colour; B: similar to dorsal colour; C: piebald pattern); shoulder spot (SS), with three character-states (A: conspicuous white spot; B: no white spot; C: faint white spot); white flank stripes (FS), with three character-states (A: flank stripe close to the wing membrane; B: flank stripe more dorsally located; C: no flank stripe); inner margin of tragus (IMT), with two character-states (A: straight; B: strongly concave); outer margin of tragus (OMT), with four character-states (A:

convex; B: slightly convex; C: circular; D: straight); tragus colour (TC), with four character-states (A: brown; B: pale; C: dark brown; D: black); ears colour (EC), with two character-states (A: identical to that of the tragus; B: different); and skull profile (SP), with four character-states (A: strongly concave; B: concave; C: weakly concave; D: straight).

Continuous and categorical variables were analysed together using the Factor Analysis of Mixed Data (FAMD) method in the FactoMineR package (Lê et al. 2008) in R version 3.2.1. (R Core Team 2015).

DNA extraction, amplification, sequencing

Total genomic DNA was extracted from muscle or patagium samples (preserved in 95% ethanol) using QIAGEN DNeasy Tissue Kit (Qiagen, Hilden, Germany) following the manufacturer's protocol with a final elution of 100 µl.

Three mitochondrial genes were sequenced for this study: the 5' fragment of the *CO1* gene, the complete cytochrome b (*Cytb*) gene, and the 5' fragment of the 12S rRNA gene (*12S*). The primers used for PCR amplification of mitochondrial genes were UTyrLA and C1-L705 for *CO1* (Hassanin et al. 2012), CB-GLU-CH2 and CB-LTHR-CH for *Cytb* (Hassanin, 2014) and 12S-U1230M2-CH (5'-GCA-CTG-AAA-ATG-CYT-AGA-TG-3') and 12S-L2226M1 (Hassanin et al. 2012) for *12S*. Four nuclear genes were sequenced for a subset of samples: intron 10 of *HDAC2* (histone deacetylase 2), intron 6 of *RIOK3* (RIO kinase 3), intron 6 of *ZFYVE27* (zinc finger, FYVE domain containing 27), and the recombination activating gene 2 (*RAG2*). The primers used for amplifying the nuclear introns are detailed in Hassanin et al. (2013), those used for *RAG2* were specifically designed for this study: RAG2-CHU (5'-CTT-CGC-TAC-CCA-GCC-ACT-TGC-A-3') and RAG2-CHL (5'-GGC-AGG-CTT-GTT-TAG-CTC-AGT-TG-3'). Amplifications were done in 20 µl using 3 µl of Buffer 10X with MgCl2, 2 µl of dNTP (6.6 mM), 0.12 µl of Taq DNA polymerase (2.5 U, Qiagen, Hilden, Germany) and 0.5-1 µl of the two primers at 10 µM. The PCRs were run using the C1000 Touch thermal cycler (BIO-RAD,

Hercules, California, USA) with the following standard conditions: 4 min at 94 °C; 5 cycles of denaturation/annealing/extension with 45 s at 94°C, 1 min at 60°C and 1 min at 72°C, followed by 30 cycles of 30 s at 94°C, 45 s at 55°C, and 1 min at 72°C, followed by 10 min at 72°C. PCR products were resolved by electrophoresis on a 1.5% agarose gel stained with ethidium bromide and visualized under UV light. Both strands of PCR products were sequenced by Eurofins MWG Operon (Ebersberg, Germany) on an ABI 3730 DNA Analyzer (Applied Biosystems, Foster City, California, USA). The sequences were edited and assembled using Sequencher 5.1 (Gene Codes Corporation, Ann Arbor, Michigan, USA). Heterozygous positions (double peaks) were scored using the IUPAC ambiguity codes. Sequences generated for this study were deposited in the GenBank database (accession numbers XXXXX- XXXXXX; for more details see **Table S1**).

Phylogenetic analyses of the mtDNA data sets

The phylogeny of *Glauconycteris* was initially analysed using 116 specimens and three mitochondrial genes (*CO1*, *Cytb* and *12S*) in order to allow comparisons with all published mtDNA sequences of *Glauconycteris*. The 101 *CO1*, 99 *Cytb*, and 96 *12S* sequences newly generated in this study were compared to 10 *CO1*, 5 *Cytb*, and 7 *12S* sequences downloaded from GenBank (for more details see **Table S1**). To identify the sister-group of *Glauconycteris*, we included 20 outgroup taxa representing a large diversity of Vespertilionidae and, in particular, all genera previously found closely related to *Glauconycteris* in molecular studies (Hoofer and Van Den Bussche 2003; Roehrs et al. 2011; Koubínová et al. 2013). DNA sequences were aligned automatically using MUSCLE (Edgar 2004) and then manually on Seaview 4.4.0 (Gouy et al. 2010). The four data sets used for mtDNA analyses were *CO1* (111 specimens and 705 nt), *Cytb* (104 specimens and 1,140 nt), *12S* (103 specimens and 959 nt), and the concatenation of the three genes, named *mtDNA-116T* (116 specimens and 2,804 nt). All trees were rooted with the genus *Myotis*, in agreement with previous molecular studies (e.g. Hoofer and Van Den Bussche 2003; Koubínová et al. 2013).

The Bayesian method was used to reconstruct phylogenetic relationships. The best-fitting model of sequence evolution was selected under jModelTest 2.1.7 (Darriba et al. 2012) using the Akaike Information Criterion (AIC). Bayesian inferences were then conducted on MrBayes v3.2.1 (Ronquist et al. 2012) using the selected GTR+G+I model for *CO1*, *Cytb*, *12S*, and *mtDNA-116T* data sets. To account for the combination of markers with contrasted molecular properties, we applied a partitioned approach using different models for *12S*, and each of the three codon-positions of the two protein genes *CO1* and *Cytb*. The posterior probabilities (PP) were calculated using four independent Markov chains run for 10,000,000 Metropolis-coupled MCMC generations, with trees sampled every 1000 generations, and a burn-in of 25%.

The results obtained from the separate Bayesian analyses of the three mtDNA markers (**Figure S1**) were also analysed for congruence using the SuperTRI method (Ropiquet et al. 2009). The lists of bipartitions obtained from the three Bayesian analyses of mtDNA genes were transformed into a weighted binary matrix for supertree construction using SuperTRI v.57 (available at http://www.normalesup.org/bli/Programs/programs.html). Each binary character corresponds to a node, which was weighted according to its frequency of occurrence in one of the three lists of bipartitions. In this manner, the SuperTRI method takes into account both principal and secondary signals, because all phylogenetic hypotheses found during the three separate analyses are represented in the weighted binary matrix used for supertree construction. The reliability of the nodes was assessed using three different measures. The first value is the Supertree Bootstrap Percentage (SBP), which was calculated under PAUP* v.4b10 (Swofford 2003) after 1000 BP replicates of the weighted binary matrix reconstructed with SuperTRI (2,038 characters; heuristic search). The second value is the ‘‘Mean Posterior Probability’’ (MPP) calculated using the lists of bipartitions obtained from Bayesian analyses of the three mtDNA data sets. The third value is the index of reproducibility (Rep), which is the ratio of the number of data sets supporting the node of interest to the total number of data sets. The MPP and Rep values

were directly calculated on SuperTRI v.57. All SuperTRI values were reported on the Bayesian tree obtained from the analysis of the *mtDNA-116T* data set.

Phylogenetic analyses based on five independent data sets

The phylogeny of *Glauconycteris* was further investigated using a reduced sample of 69 individuals (including 54 *Glauconycteris*) sequenced for multiple loci, including four nuclear genes (*HDAC2*, *RIOK3*, *ZFYVE27*, and *RAG2*) and a concatenation of the three mtDNA genes *CO1*, *Cytb* and *12S*. It was not possible to include the species *G. poensis* in these analyses, because the quality of the DNA extracted from specimens DM 14186, DM 14187, and DM 14188 was not sufficient to obtain successful amplification of nuclear markers. The nuclear analyses were performed to test possible discordance between the phylogenetic signals extracted from independent markers, and to avoid misleading taxonomic interpretations due to either mtDNA introgression, lineage sorting, or different dispersal behaviour between females and males (e.g. Nesi et al. 2011; Hassanin et al. 2015). A few gaps were included in the alignments of the nuclear introns, but their positions were not found to be ambiguous. The indels shared by at least two individuals were coded as additional characters ("1": insertion; "0": deletion) and analysed as a separate partition in the Bayesian analyses.

A total of seven data sets were analysed: (1) supermatrix, combining all the seven genes (6,124 nt + 55 indels); (2) *nuDNA*, combining all the four nuclear genes (3,320 nt + 55 indels); (3) *mtDNA-69T*, combining the three mtDNA genes (2,804 nt); (4) *HDAC2* (888 nt + 20 indels); (5) *RIOK3* (656 nt + 17 indels); (6) *ZFYVE27* (759 nt + 18 indels); and (7) *RAG2* (1,017 nt). The Bayesian analyses were performed as detailed above for mitochondrial data sets. The following models of nucleotide evolution were selected under jModelTest using ACI: GTR+G+I for *mtDNA-69T* and *RAG2*, GTR+G for *HDAC2*, and HKY+G for *RIOK3* and *ZFYVE27*. The results obtained from the separate Bayesian analyses of the five independent data sets (*mtDNA-69T* and the four nuclear genes; **Figure S2**) were also analysed for congruence using the SuperTRI

method (Ropiquet et al. 2009), and the reliability of the nodes was assessed using SBP (weighted binary matrix = 2,693 characters), MPP, and Rep values (see above for details). All SuperTRI values were reported on the Bayesian tree obtained from the *nuDNA* analysis.

Molecular dating

Divergence times were estimated with the Bayesian approach implemented in BEAST v.2.1.3 (Bouckaert et al. 2014). As no fossil record or biogeographic event is available for *Glauconycteris*, we employed two different strategies for molecular dating: the first one is based on *Cytb* haplotypes (77 sequences and 1,140 nt) and *a priori* assumptions on the rate of substitutions; the second one is based on *RAG2* sequences from a large diversity of Vespertilionidae (126 sequences and 1,017 nt) and the use of several calibration points. In agreement with published data on the nucleotide substitution rates in the *Cytb* of mammals (Arbogast and Slowinski 1998), we tested two substitution rates for estimating divergence times with the *Cytb* alignment: R1 = 0.02 ± 0.005 and R2 = 0.025 ± 0.005 per site per lineage per Myr. For the *RAG2* alignment, we used three molecular calibration points extracted from the studies of Teeling et al. (2005) and Meredith et al. (2011): 10 ± 3 Mya for the most recent common ancestor (MRCA) of *Antrozous* and *Rhogeessa*; 20.5 ± 4.5 Mya for the MRCA of *Myotis* and *Antrozous*; and 46 ± 5 Mya for the MRCA of *Myotis* and *Miniopterus*. In agreement with Lack et al. (2010), the *RAG2* tree of the family Vespertilionidae was rooted with *Cistugo seabrae* (Cistugidae) and *Miniopterus inflatus* (Miniopteridae).

For all analyses, we applied a GTR+G+I model of evolution (based on jModelTest) for each of the three codon-positions of *Cytb* or *RAG2* genes, and a relaxed-clock model with uncorrelated lognormal distribution for substitution rates. Node ages were estimated using a Yule speciation prior and 10^8 generations, with tree sampling every 1000 generations, and a burn-in of 10 %. Adequacy of chain mixing and MCMC chain convergence were assessed using the ESS values in Tracer v.1.6 (available in the BEAST package). The chronograms were generated with

TreeAnnotator v.1.8.2 (available in the BEAST package) and visualized with FigTree v.1.4.1 (http://tree.bio.ed.ac.uk/software/).

RESULTS

Taxonomic identifications

In the DRC, we caught 52 individuals of *Glauconycteris*, including 29 females and 23 males. We identified seven species at different localities on the left bank [L] and/or right bank [R] of the Congo River: *G. alboguttata* (four individuals; Melume [R]), *G. argentata* (11 individuals; Yoko [L]; Melume [R], Mbiye [R], and Sukisa [R]), *G. curryae* (five individuals; Yaengo [L], Yatolema [L], and Yoko [L]), *G. superba* (11 individuals; Yoko [L] and Mbiye [R]), and three species within the *beatrix*/*humeralis* morpho-group (22 individuals; seven localities), i.e. a first species identified as *G. beatrix*, which is represented by 16 dark sepia brown bats with faint white shoulder spots (Yatolema [L], and Yoko [L]; Bongandjolo, Mbiye [R], Melume [R], and Sukisa [R]); a second species identified as *G. humeralis*, characterized by smaller forearm and tibia lengths than females of *G. beatrix* (FA=35.6 *versus* 36.9-39.5; TIB=16.4 *versus* 18.8-20.1), a more reddish brown colour, and the presence of conspicuous white shoulder spots (rather than faint white shoulder spots in *G. beatrix*), which is represented by one female collected at Sukisa [R]; and a third species, which is described below, represented by five blackish brown bats without white markings (Yaengo [L], Yatolema [L], and Yoko [L]).

Our analyses also include 26 individuals of *Glauconycteris* collected in Dzanga-Sangha (southern CAR; code "R13"), representing five species, i.e. *G. alboguttata* (eight individuals), *G. curryae* (one individual), *G. egeria* (six individuals), *G. beatrix* (three individuals with TIB > 19), and *G.* cf. *humeralis* (two females with TIB < 18 and a conspicuous white spot on each shoulder); one male of *G. egeria* from Mbaéré-Bodingué (southern CAR; R08-61); three individuals of *G. poensis* from Liberia (DM14186 - DM14188) (reported in Monadjem et al. 2016); five individuals of *G. variegata* from Botswana (ECJS-43/2009), South Africa (TM 48494

- TM 48496), and Zambia (ECJS-92/2010); and one female from Cameroon (HNHM 23262) identified as *G. beatrix* (FA=39.0; TIB=20.1), which is characterized by the absence of white markings.

For all nine species identified in DRC and CAR, we found that females have longer forearms than males (**Figure S3**). A female-biased size dimorphism was also observed for other measurements, such as the tibia length and weight (data not shown).

Systematic description

Glauconycteris atra sp. nov.

Holotype: MNHN 2016-2792 (field number: K13-215), adult female, in alcohol, skull removed, collected on 05 December 2013 by AH, GCG, PMA, RC, TG, and VTT. The holotype was used in the molecular and morphological comparisons presented herein. W: 8.5 g; FA: 37.8; Tib: 17.9; T: 42.6; HB: 55.8; F1: 4.4; 2DM: 37.3; 3DM: 38.8; 3D1P: 13.8; 3D2P: 23.0; 4DM: 36.5; 5DM: 34.2; GLS: 12.63; ZW: 9.34; BCW: 7.49; IOW: 4.61; MB: 8.15; BCH: 7.66; LWP: 2.56; M_3-M_3: 4.05; C_1-C_1: 2.54; C-M_3: 4.20; C-M^3: 4.45; M^3-M^3: 5.87; C^1-C^1: 4.35; ML: 8.63; MW: 7.31 mm. Accession numbers of mitochondrial and nuclear sequences are MF038602 (*CO1*), MF038501 (*Cytb*), MF038702 (*12S*), MF038428 (*HDAC2*), MF038290 (*RIOK3*), MF038359 (*RAG2*), and MF038222 (*ZFYVE27*).

Type locality: Yaengo, Tshopo Province, Democratic Republic of the Congo: 0.34887°N; 24.48200°E; 400 m above sea level (a.s.l.).

Referred specimens: One additional individual from Yaengo (MNHN 2016-2791: adult male); two individuals from Yatolema (0.41319°N; 24.53908°E; 460 m a.s.l.; MNHN 2016-2790:

adult male; MNHN 2016-2793: adult female); and one individual from Yoko (0.29410°N; 25.28895°E; 412 m a.s.l.; MNHN 2016-2794: adult female). Accession numbers of mitochondrial and nuclear sequences are detailed in Appendix 1.

Etymology: The specific epithet refers to the pelage colour, which is dark and gloomy (blackish brown) without any white markings (**Figure 2**). We propose 'Blackish Butterfly Bat' as the English common name and '*Glauconyctère sombre*' as the French common name.

Diagnosis: A small-sized species of *Glauconycteris* with a forearm length between 34.4 and 37.8 mm (n=5), with some evidence of sexual dimorphism, as males tend to be slightly smaller than females (**Figure S3**). It has a stocky build, with a weight range of 8.5-8.7 g for females (n=3) and 6.9-7.7 g for males (n=2), which is much heavier than other small-sized species of *Glauconycteris* collected in northeastern DRC, such as *G. beatrix* (3.9-6.1 g; n=10), *G. curryae* (3.6-5.0 g; n=5), and *G. humeralis* (4.7 g; n=1). The dorsal pelage colour of the living animal is blackish brown without any white markings. The ventral pelage is paler. Dorsally, the fur extends onto the plagiopatagium along the proximal half of the humerus and femur and onto the uropatagium along the proximal half of the tail. The two males are darker in colour than the three females (**Figure 2**). The sexual dimorphism in pelage colour, however, needs to be confirmed by observations of additional specimens. Dorsal hairs are 6-8 mm long and tricoloured: dark brown at the base, beige in the middle and blackish brown at the tip. The wings, interfemoral membrane, ears, and naked skin around muzzle and eyes are blackish brown. The inner margin of the tragus is straight or slightly curved, whereas the outer margin of the tragus is well rounded (**Figure 2**). Although similar in appearance to other species of *Glauconycteris*, the skull of *G. atra* sp. nov. is larger than in related species, such as *G. beatrix*, *G. curryae*, and *G. humeralis*, with little overlap in the different measurements (MW, ZW, BCW, MB). In addition, the braincase is relatively higher (BCH) (see in **Table S2**).

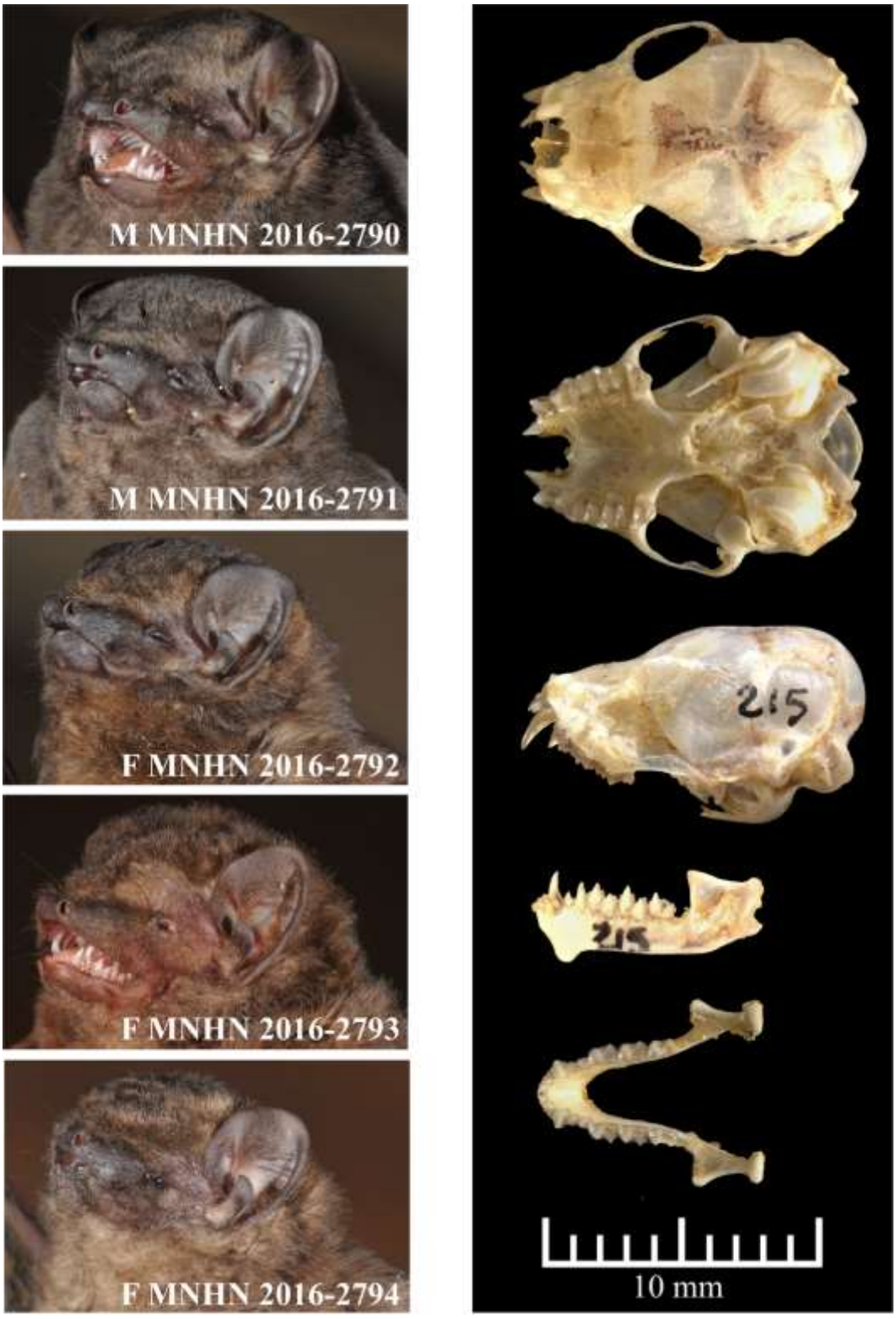

Figure 2. *Glauconycteris atra* sp. nov.

Left column: portraits of the five individuals of *Glauconycteris atra* sp. nov. (F: female; M: male) collected in the Tshopo Province of the Democratic Republic of the Congo (photographs taken by AH).

Right column: skull views of the holotype of *Glauconycteris atra* sp. nov. MNHN 2016-2792 (field number: K13-215) (High-dynamic-range photographs taken by Alexandre Hanquet, UMS 2700 MNHN).

Description: Based on pelage coloration, *G. atra* sp. nov. cannot be confused with any other known species of *Glauconycteris*. It lacks the conspicuous body patterns of white spots, white stripes or reticulated wings found in most other species of *Glauconycteris*. Its general colour is much darker than the sepia- or reddish-brown colours of *G. beatrix*, *G. curryae*, and *G. humeralis*. The forearm length of *G. atra* sp. nov. ranges from 36.1 to 37.8 mm in females (n=3) and from 34.5 to 36.8 mm in males (n=2), which is similar to *G. curryae* and *G. humeralis*, but slightly smaller than *G. beatrix* (**Figure S3**). The tibia length ranges from 17.2 to 17.9 mm in females (n=3) and from 16.3 to 17.2 mm in males (n=2), which is similar to *G. curryae*, but slightly smaller than *G. beatrix*, and slightly larger than *G. humeralis*. The tail is shorter than HB. The ears are separated, short (10–11 mm) and rounded. In lateral view, the skull profile of the forehead region is moderately concave in *G. atra* sp. nov., as observed in *G. humeralis* and some individuals of *G. beatrix*. By contrast, the profile is strongly concave in *G. curryae*. The dental formula of *G. atra* sp. nov. is I 2/3 C 1/1 P 1/2 M 3/3 = 32 teeth, which is identical to that of other *Glauconycteris* species. The inner upper incisors are strongly bicuspid with the outer cusp smaller than the inner cusp, as observed in *G. beatrix*, *G. curryae*, and *G. humeralis*. The inner lower incisors have three cusps, whereas the two outer incisors have four cusps.

Distribution and natural history: All five specimens of *G. atra* sp. nov. were caught in riparian zones on the left bank of the Congo River, at three localities of the Tshopo Province of the Democratic Republic of the Congo: Yaengo, Yatolema, and Yoko. The new species was found in sympatry with *G. argentata* (Yoko), *G. beatrix* (Yatolema and Yoko), *G. curryae* (Yaengo and Yatolema) and *G. superba* (Yoko).

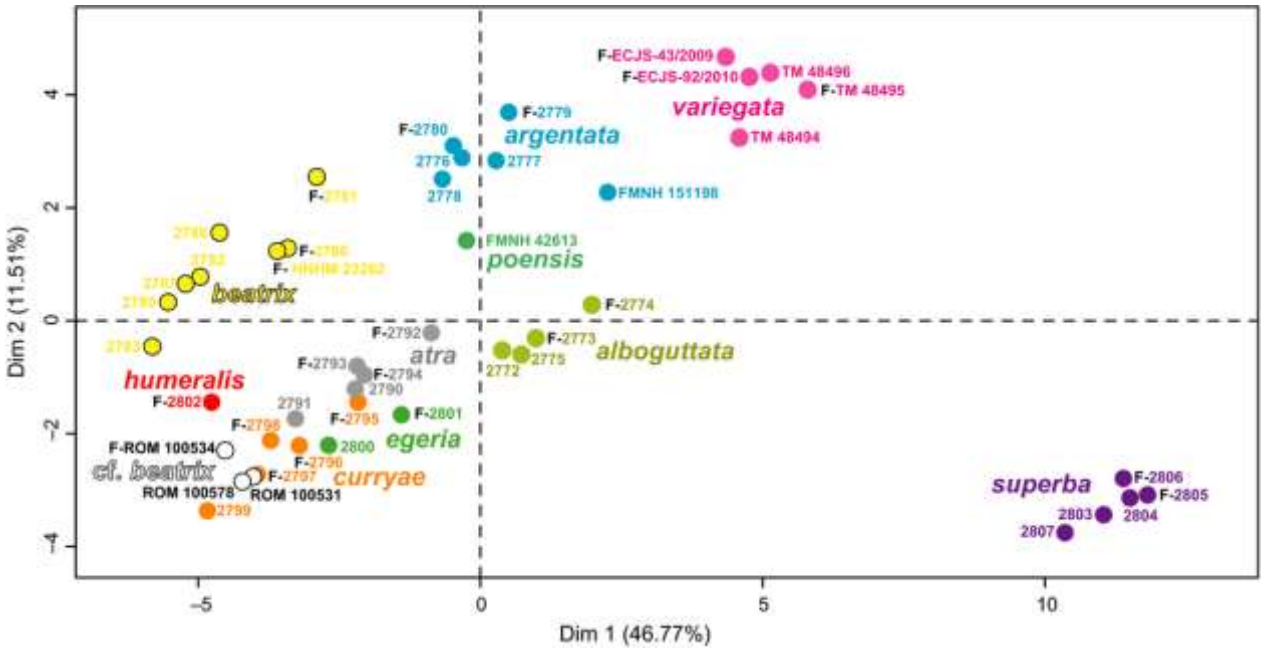

Figure 3. Plot obtained from the morphological analysis of 45 specimens of *Glauconycteris*.

The plot of Dimension 1 against Dimension 2 was obtained from the Factor Analysis of Mixed Data (FAMD) in the FactoMineR package. The 26 quantitative and 11 qualitative variables used for the analysis are detailed in the Materials and Methods and **Table S2**.

The individuals are named with the codes detailed in **Table S1**, the prefix "F" indicates females. For MNHN specimens, the first part of the code (i.e., MNHN 2016-) was not indicated to facilitate the reading of the figure.

Morphological analyses

We examined 45 adult specimens, representing 11 species, for which we measured 26 quantitative variables and coded 11 qualitative variables (**Table S2**). Using the FAMD method, the dimensions 1, 2, 3, 4 and 5 account for 46.8%, 11.5%, 8.8%, 7.2%, and 6.5% of total variance, respectively. The plot of Dimension 1 against Dimension 2 (**Figure 3**) shows the existence of several clusters corresponding to *G. superba*, *G. variegata*, *G. argentata*, *G. alboguttata*, *G. beatrix*, and *G. poensis*. By contrast, these two dimensions cannot be used to distinguish individuals of *G. atra* sp. nov. from *G. curryae*, *G.* cf. *beatrix*, and *G. egeria*. Several specimens housed in the ROM identified as *G. beatrix* are hereafter referred to as. *G.* cf. *beatrix* as they do not plot with other *G. beatrix*, and overlap instead with individuals of *G. curryae*.

Most variables contribute to the construction of Dimension 1, whereas Dimension 2 is mainly explained by the quantitative variable 18 (tail length) and the qualitative variable q11 (skull profile).

The morphological analysis based only on similar smaller forms (i.e., discarding the obviously different species: *G. alboguttata*, *G. argentata*, *G. poensis*, *G. superba*, and *G. variegata*) did not improve the discrimination between these closely related species (data not shown).

Mitochondrial phylogeny

The Bayesian tree obtained from the concatenation of the three mitochondrial genes (*CO1*, *Cytb* and *12S*; 116 specimens and 2,804 nt) is shown in **Figure 4**. In the total alignment, the missing data represent 9.5%, because we included 13 additional individuals of *Glauconycteris* from GenBank, for which no sequence was available for one or two mitochondrial genes (see **Table S1** for details). Most of the nodes are supported by high values of posterior probabilities (PP = 0.9-1) and high SuperTRI values (SBP ≥ 80, MPP ≥ 0.5, Rep ≥ 0.7). As expected, the nodes containing one or several specimens with missing data have lower values of SBP. For instance, the sister-group relationship between individuals of *G. egeria* (R08-61 and AMNH 268381) was supported by SBP = 40, because only the *12S* gene was sequenced for the AMNH specimen.

The monophyly of the genus *Glauconycteris* was strongly supported by the analyses, as well as that of the three other genera of Vespertilionidae for which at least two species were included in the data set, i.e. *Arielulus*, *Eptesicus*, and *Hesperoptenus* (PP = 1; SBP = 87-100; MPP = 0.7-1; Rep = 0.7-1). Four intergeneric relationships were supported by PP = 1 and by at least two mitochondrial genes (Rep ≥ 0.7): (1) *Glauconycteris* + *Hesperoptenus*; (2) *Ia* + *Scotomanes*; (3) *Chalinolobus* + *Laephotis*, and (4) their association with *Mimetillus*.

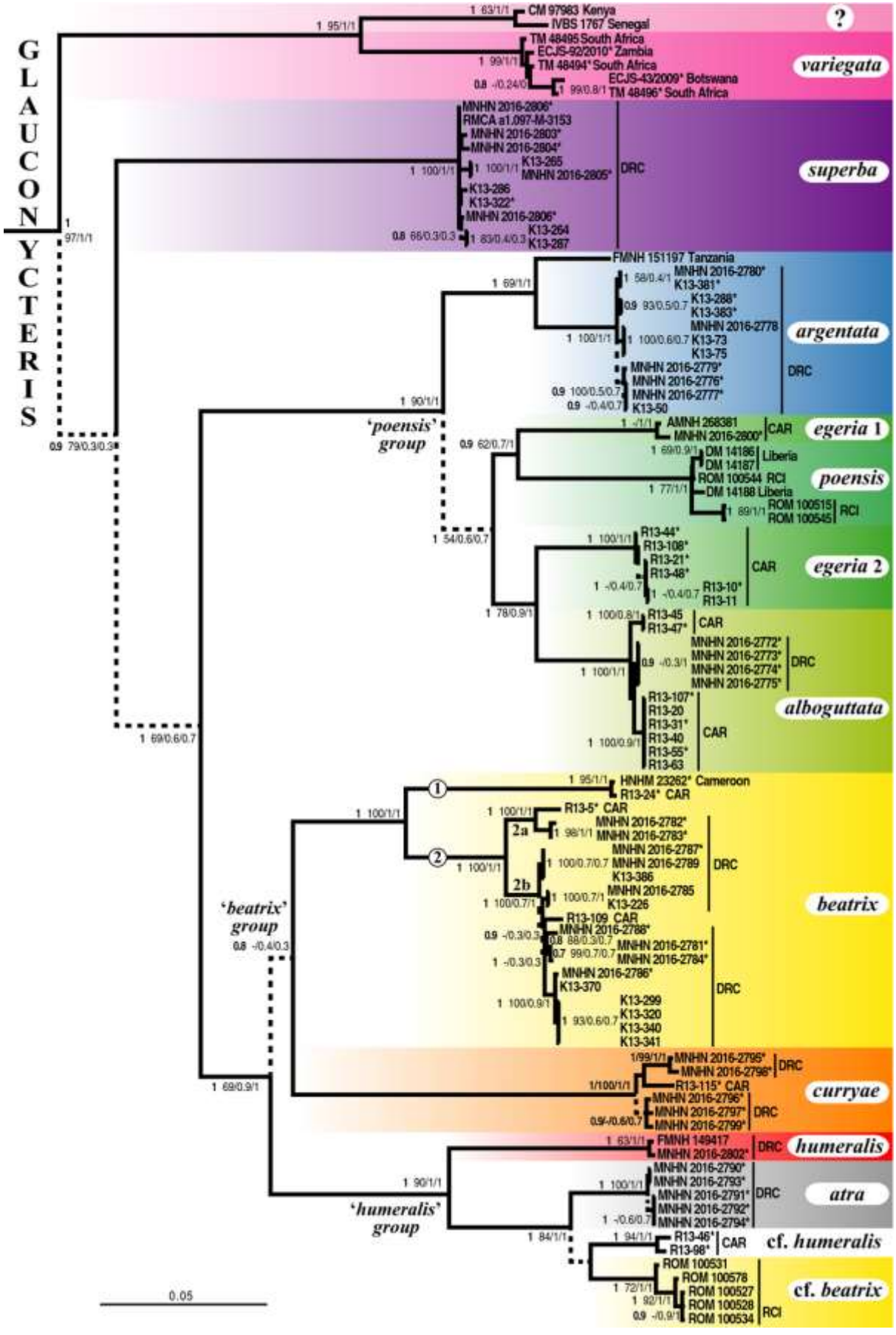
GLAUCONYCTERIS
?
variegata
CM 97963 Kenya
IVBS 1767 Senegal
TM 48495 South Africa
ECJS-92/2010* Zambia
TM 48494* South Africa
ECJS-43/2009* Botswana
TM 48496* South Africa
superba
MNHN 2016-2806*
RMCA a1.097-M-3153
MNHN 2016-2803*
MNHN 2016-2804*
K13-265
MNHN 2016-2805*
K13-286
K13-322*
MNHN 2016-2806*
K13-264
K13-287
DRC
argentata
FMNH 151197 Tanzania
MNHN 2016-2780*
K13-381*
K13-288*
K13-383*
MNHN 2016-2778
K13-73
K13-75
MNHN 2016-2779*
MNHN 2016-2776*
MNHN 2016-2777*
K13-50
DRC
'poensis' group
egeria 1
AMNH 268381
MNHN 2016-2800*
CAR
poensis
DM 14185
DM 14187
Liberia
ROM 100544 RCI
DM 14188 Liberia
ROM 100515
ROM 100545
RCI
egeria 2
R13-44*
R13-108*
R13-21*
R13-48*
R13-10*
R13-11
CAR
alboguttata
R13-45
R13-47*
CAR
MNHN 2016-2772*
MNHN 2016-2773*
MNHN 2016-2774*
MNHN 2016-2775*
DRC
R13-107*
R13-20
R13-31*
R13-40
R13-55*
R13-63
CAR
'beatrix' group
beatrix
HNHM 23262* Cameroon
R13-24* CAR
R13-5* CAR
MNHN 2016-2782*
MNHN 2016-2783*
MNHN 2016-2787*
MNHN 2016-2789
K13-386
MNHN 2016-2785
K13-226
DRC
R13-109 CAR
MNHN 2016-2788*
MNHN 2016-2781*
MNHN 2016-2784*
MNHN 2016-2786*
K13-370
K13-299
K13-320
K13-340
K13-341
DRC
curryae
MNHN 2016-2795*
MNHN 2016-2798*
DRC
R13-115* CAR
MNHN 2016-2796*
MNHN 2016-2797*
MNHN 2016-2799*
DRC
humeralis
FMNH 149417
MNHN 2016-2802*
DRC
'humeralis' group
atra
MNHN 2016-2790*
MNHN 2016-2793*
MNHN 2016-2791*
MNHN 2016-2792*
MNHN 2016-2794*
DRC
cf. humeralis
R13-46*
R13-98*
CAR
cf. beatrix
ROM 100531
ROM 100578
ROM 100527
ROM 100528
ROM 100534
RCI
0.05

Figure 4. Mitochondrial tree inferred from the concatenation of *CO1*, *Cytb*, and *12S* genes.

The Bayesian tree was reconstructed using 116 specimens (including 96 individuals of *Glauconycteris*) and the concatenation of three mitochondrial genes (*CO1*, *Cytb*, and *12S*; 2,804 nt). The values in bold at internal branches represent the posterior probabilities calculated with the mitochondrial concatenation. The three other values were obtained from the SuperTRI analyses of the three mitochondrial genes: from left to right, Supertree Bootstrap percentage (SBP), Mean posterior probability (MPP), and Reproducibility index (Rep). The symbol "-" indicates that the node was not found in the analysis, and that no alternative hypothesis was supported by PP > 0.7. Dash branches highlight nodes that were not found monophyletic with each of the three mitochondrial genes (Rep ≤ 0.7). At terminal branches, all sample codes are followed by the country of origin (Abbreviations: CAR = Central African Republic; RCI = Republic of Côte d'Ivoire; DRC = Democratic Republic of the Congo). A map of geographic localities is provided in **Figure S7**. The individuals with an asterisk (*) were also sequenced for four nuclear genes (see **Figure 5**).

Within *Glauconycteris*, our analyses revealed the existence of three major clades: (1) *G. variegata*; (2) *G. superba*; and (3) a clade uniting all other species, which can be further divided into four robust groups: (i) the '*poensis'* group, which includes *G. poensis*, *G. alboguttata*, *G. argentata*, and *G. egeria* 1 and 2; (ii) *G. beatrix* from Central Africa (Cameroon, CAR and DRC); (iii) *G. curryae*; and (iv) the '*humeralis*' group, which contains *G. humeralis* and *G. atra* sp. nov. in DRC, *G.* cf. *humeralis* in CAR, and *G.* cf. *beatrix* in Republic of Côte d'Ivoire (RCI).

Most species were found to be monophyletic with PP = 1 and Rep = 1 (i.e. supported by the three mtDNA markers), with the exception of *G. beatrix*, *G. egeria*, and *G. humeralis*. The species *G. egeria* splits into two unrelated haplogroups. The first haplogroup, named *G. egeria* 1, contains two individuals from CAR (AMNH 268381 from Dzanga-Sangha; R08-61 from Mbaéré Bodingué National Park) (PP = 1; SBP = 40; MPP/Rep = 1). It appears as the sister-group of *G. poensis* (PP = 0.9; SBP = 62; MPP = 0.7; Rep = 1), from which it differs by 6.5-8.0 % in *CO1* sequences and 10 % in *Cytb* sequences. The second haplogroup, named *G. egeria* 2, is composed of all other individuals collected in Dzanga-Sangha (PP = 1; SBP = 100; MPP/Rep = 1). It appears as the sister-group of *G. alboguttata* (PP = 1; SBP = 78; MPP = 0.9; Rep = 1), from

which it differs by 5.8-6.2% in *CO1* sequences, 5.8-6.6 % in *Cytb* sequences, and 2.3-2.6 % in *12S* sequences. Highly divergent mitochondrial haplogroups were also detected in several other species. In *G. variegata*, there are two geographic haplogroups separated by more than 10.3 % in *Cytb* and 4.2 % in *12S*. The first haplogroup includes the individuals collected in southern Africa (Botswana, South Africa and Zambia), and the second contains two individuals from two widely spaced localities in East and West Africa (CM 97983: Kenya; IVBS 1767: Senegal). In *G. argentata*, the *12S* sequence from an individual from Tanzania (FMNH 151197) was found to be > 2.2% distant from that of individuals collected in DRC. In *G. beatrix* sensu stricto (s.s.), i.e. from Central Africa, there are two highly divergent haplogroups (*CO1*: > 9.4%; *Cytb*: > 8.7%; *12S*: > 2.8%): the first is only represented by two individuals, i.e. one from Cameroon (HNHM 23262) and another one from CAR (R13-24); and the second includes a few individuals from CAR and all the individuals collected in eastern equatorial Africa (DRC). The second haplogroup of *G. beatrix* s.s. can be subdivided into two subgroups, named 2a and 2b in **Figure 4** (*CO1*: >2.6%; *Cytb*: > 2.3%; *12S*: >1.2%).

In the '*humeralis*' group, there are three geographic haplogroups corresponding to *G. atra* sp. nov. (DRC), *G.* cf. *beatrix* (RCI), and *G.* cf. *humeralis* (CAR) (*CO1*: >4.2%; *Cytb*: > 4.6%; *12S*: >3.1%), which are highly distinct from the two specimens from DRC assigned to the species *G. humeralis* (K13-47 and FMNH 149417, highlighted in red in **Figure 4**) (*CO1*: > 9.2%; *Cytb*: > 11.7%; *12S*: > 4.6%).

Nuclear, Supermatrix and SuperTRI analyses

The Bayesian tree obtained from the concatenation of the four nuclear genes *HDAC2*, *RAG2*, *RIOK3*, and *ZFYVE27* (*nuDNA*; 69 specimens and 3,375 characters; missing data = 1.8%) is shown in **Figure 5**, while the Bayesian tree reconstructed with the supermatrix (all mitochondrial and nuclear genes; 69 specimens and 6,179 characters; missing data = 1.3%) is provided in **Figure S4**. The topologies are very similar to that inferred from the mtDNA data set

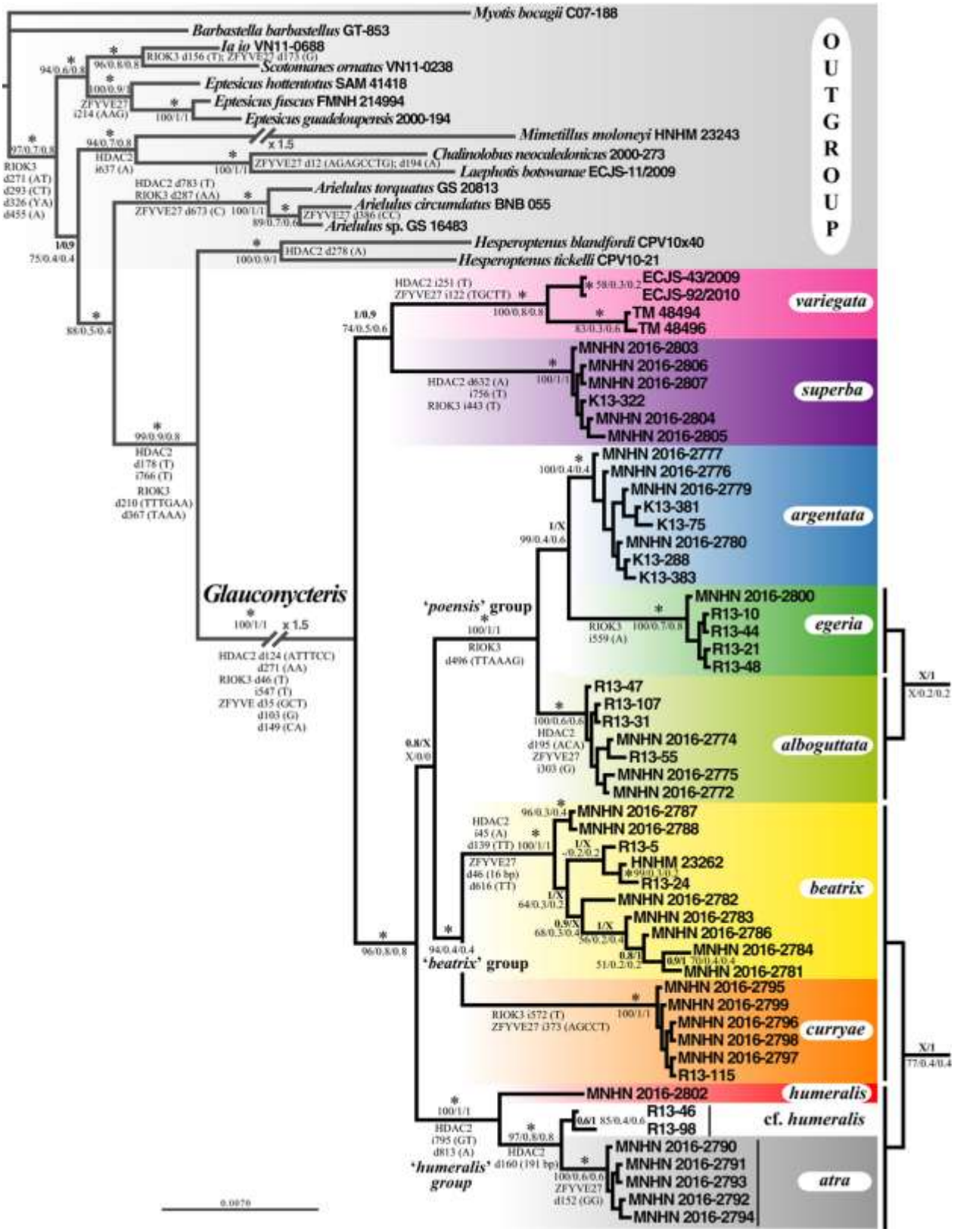

Figure 5. Nuclear tree inferred from the concatenation of *HDAC2*, *RAG2*, *RIOK3*, and *ZFYVE* genes.

The Bayesian tree was reconstructed using 69 specimens (including 54 individuals of *Glauconycteris*) and the nuclear matrix combining the four genes *HDAC2*, *RAG2*, *RIOK3*, and *ZFYVE* (3,375 characters). The branches at the right show alternative groupings found with $PP_{tot} = 1$ in the supermatrix analysis.

For each node, the two values in bold indicate posterior probabilities calculated either from the concatenation of the four nuclear genes (PP_{nu} at the left of the slash) or from the supermatrix combining all nuclear and mitochondrial genes (PP_{tot} at the right of the slash; 6,179 characters). The asterisk (*) indicates that the node was supported by maximal values of robustness ($PP_{nu/tot} = 1$). The letter ''X'' indicates that the node was not found in the analysis, and that an alternative hypothesis was supported by PP > 0.7. The three other values were obtained from the SuperTRI analyses of the five physically unlinked markers (mtDNA concatenation and the four independent nuclear genes): from left to right, Supertree Bootstrap percentage (SBP), Mean posterior probability (MPP), and Reproducibility index (Rep). The position and nature of all diagnostic indels (i: insertion; d: deletion) shared by at least two individuals in the DNA alignments of nuclear genes are also shown at the nodes.

(**Figure 4**). Most nodes of the mtDNA tree were recovered with maximal support values in the nuDNA and supermatrix (mtDNA+nuDNA) trees (PP = 1): Vespertilioninae; the monophyly of the genera *Glauconycteris*, *Arielulus*, *Eptesicus*, and *Hesperoptenus*; *Ia* + *Scotomanes*; *Chalinolobus* + *Laephotis*, and their association with *Mimetillus*; the sister-group relationship between *E. fuscus* and *E. guadeloupensis*; the monophyly of the species *G. alboguttata*, *G. argentata*, *G. beatrix* s.s., *G. curryae*, *G. variegata*, and *G. superba*; the monophyly of the '*beatrix*' group (*G. beatrix* s.s. + *G. curryae*), '*humeralis*' group (*G. humeralis* + *G. atra* sp. nov. + *G.* cf. *humeralis* + *G.* cf. *beatrix*), and '*poensis*' group (as represented by *G. alboguttata*, *G. argentata*, and *G. egeria*). Most of these nodes were supported by high values in the SuperTRI analyses of the five independent markers (mtDNA and four nuclear genes): SBP ≥ 94; MPP ≥ 0.7; and Rep ≥ 0.8. Two nodes were moderately supported: the species *G. alboguttata* (SBP = 100; MPP/Rep = 0.6), which is recovered monophyletic in the separate analyses of three independent markers (*mtDNA*, *HDAC2*, *ZFYVE27*; **Figure S2**); and the '*beatrix*' group (SBP = 94; MPP/Rep = 0.4), which was found monophyletic with only two markers (*mtDNA* and *RAG2*; **Figure S2**). A few nodes of the mtDNA tree are clearly discordant with the nuDNA topology.

The species *G. egeria*, which appeared polyphyletic in the mitochondrial tree (PP = 1), is monophyletic in the nuclear tree (PP = 1) and in all separate analyses of the four nuclear genes

(**Figure S2**). The species *G. egeria* can be also diagnosed by an insertion of A nucleotide in position 559 of the *RIOK3* alignment. Three nuclear genes indicate that it is closely related to *G. argentata* (*HDAC2*, *RAG2*, and *ZFYVE27*).

Within *G. beatrix* s.s., the nuDNA tree does not corroborate the existence of three divergent haplogroups, as shown in the mitochondrial tree (1, 2a and 2b in **Figure 4**).

Most of the poorly supported nodes of the mitochondrial tree (PP ≤ 0.9) were not recovered in the nuclear tree. The species *G. variegata*, which occupied a basal position within *Glauconycteris* in the mitochondrial tree (PP = 0.9), is the sister-species of *G. superba* in the nuclear tree (PP = 1), a result supported by the separate analyses of *HDAC2*, *RAG2* and *ZFYVE27* genes (**Figure S2**). The genus *Arielulus*, which was grouped with *Eptesicus*, *Ia* and *Scotomanes* in the mtDNA tree (PP = 0.8), is allied to *Glauconycteris* and *Hesperoptenus* in the nuclear tree (PP = 1), a result recovered in the separate analyses of *RAG2* and *ZFYVE27* genes (**Figure S2**).

The tree reconstructed from the supermatrix (**Figure S4**) is in agreement with the nuclear tree for the deepest nodes (i.e. position of *Arielulus*, *G. variegata* + *G. superba*), but it is more similar to the mitochondrial tree for the most recent nodes (e.g., *G. egeria* +*G. alboguttata*, the three haplogroups within *G. beatrix* s.s.). Most topological conflicts between nuclear and supermatrix trees can be resolved using the results from SuperTRI analyses. The topology of the SuperTRI Bootstrap 50% majority-rule consensus tree (data not shown) is identical to the nuclear tree, except some unsupported nodes at the intra-specific levels. The SuperTRI analyses also support the placement of *Arielulus* as sister-group of the clade uniting *Glauconycteris* and *Hesperoptenus* (SBP = 88; MPP = 0.5; Rep = 0.4), and the sister-group relationship between *G. superba* and *G. variegata* (SBP = 74; MPP = 0.5; Rep = 0.6). In agreement with the nuclear tree, the SuperTRI analyses favour the association between *G. egeria* and *G. argentata* (SBP = 99; MPP = 0.4; Rep = 0.6). In addition, they do not confirm the existence of three haplogroups within

G. beatrix s.s., as most intra-specific relationships are associated to low MPP and Rep values (≤ 0.4).

Molecular dating of *Glauconycteris*

Two data sets were used for molecular dating: an alignment of 126 *RAG2* sequences, which is more appropriate to estimate the deeper nodes of our phylogeny; and an alignment of 77 *Cytb* haplotypes, which contains a large diversity of *Glauconycteris* sequences, and which is therefore more accurate to estimate the most recent divergence times. The *Cytb* alignment was analysed with two different rates of substitution, R1 = 0.02 ± 0.005 and R2 = 0.025 ± 0.005 per site per lineage per Myr. The three chronograms *RAG2*, *Cytb* R1, and *Cytb* R2 are available in **Figure S5**. For nodes in common, we found that the *RAG2* ages estimated with three calibration points were systematically younger than the *Cytb* ages estimated using either R1 or R2 substitution rates. These comparisons suggest that the faster *Cytb* R2 rate was more reliable than the slower *Cytb* R1 rate. In **Table 1**, we therefore only show the ages estimated with *RAG2* and *Cytb* R2. The 95% intervals were found to be generally larger for *RAG2* ages, because the *RAG2* data set was analysed using three calibration points (10, 20.5 and 46 Mya) older than the MRCA of the ingroup and with large standard deviations (between 3 and 5 Mya).

Our results indicate that *Glauconycteris* diverged from *Hesperoptenus* during the Middle/Late Miocene at around 10 ± 3 Mya, and then it diversified into three main lineages (*G. superba*, *G. variegata*, and the clade uniting all other species) at the end of the Miocene at around 6 ± 2 Mya. All other speciation events occurred during the Pliocene and up until the Early Pleistocene. Divergence times at the species level were estimated between the Middle and Late Pleistocene, with the exception of *G. beatrix* s.s. (Early Pleistocene), and the separation between northern and southern groups of *G. variegata* (Early Pleistocene).

Table 1. Bayesian mean node ages (and 95% intervals) in million years ago estimated with either *RAG2* or *Cytb* datasets (see Figure S5 for chronograms)

Taxa	***RAG2***	***Cytb*R2**	**Epochs**
1. R2 = .025 ± .005 per lineage/Myr; NA, not applicable			
Interspecific relationships			
Glauconycteris + *Hesperoptenus* + *Arielulus*	12.61 (16.7–8.7)	10.98 (14.4–8.0)	Middle Late Miocene
Glauconycteris + *Hesperoptenus*	10.93 (14.9–7.1)	10.25 (13.6–7.4)	Middle Late Miocene
Genus *Arielulus*	4.48 (8.4–1.3)	6.36 (8.8–4.1)	Miocene/Pliocene
Genus *Hesperoptenus*	7.82 (11.4–4.4)	7.02 (10.0–4.3)	Late Miocene
Genus *Glauconycteris*	5.70 (8.4–3.3)	6.32 (8.2–4.6)	Late Miocene
G. superba + *G. variegata*	3.91 (6.6–1.4)	5.60 (7.6–3.8)	Pliocene
G. superba	NA	0.19 (0.3–0.1)	Middle/Late Pleistocene
G. variegata (southern Africa + Senegal)	NA	2.44 (3.6–1.4)	Early Pleistocene
G. variegata (only southern Africa)	0.36 (1.2–0.0)	0.34 (0.5–0.2)	Middle Pleistocene
Groups "*poensis"* + "*beatrix"* + "*humeralis"*	4.19 (6.3–2.3)	5.17 (6.8–3.8)	Pliocene
Groups "*beatrix"* + "*humeralis"*	3.48 (6.3–2.3)	4.45 (5.8–3.2)	Pliocene
Group "*beatrix"*	2.87 (4.5–1.4)	3.93 (5.3–2.7)	Pliocene
G. beatrix (Central Africa)	1.89 (3.2–0.7)	2.35 (3.4–1.4)	Early Pleistocene
G. beatrix but HNHM 23262 (+ R13-24)	0.85 (1.9–0.0)	0.67 (1.0–0.4)	Middle Pleistocene
G. curryae	0.28 (0.9–0.0)	0.41 (0.6–0.2)	Middle Pleistocene
Group "*humeralis"*	1.47 (3.0–0.3)	2.61 (3.7–1.7)	Pliocene/Pleistocene
G. atra + *G.* cf. *humeralis*	0.31 (1.0–0.0)	1.02 (1.5–0.6)	Early/Middle Pleistocene
Group "*poensis"*	1.67 (3.3–0.4)	3.26 (4.4–2.3)	Pliocene/Pleistocene
G. poensis + *G. egeria* + *G. alboguttata*	NA	2.53 (3.4–1.7)	Pliocene/Pleistocene
G. argentata + *G. egeria*	0.87 (1.9–0.1)	NA	Pleistocene
G. poensis + *G. egeria*1	NA	2.21 (3.1–1.4)	Early Pleistocene
G. alboguttata + *G. egeria*2	NA	1.49 (2.2–0.9)	Early Pleistocene
G. poensis	NA	0.15 (0.3–0.0)	Middle/Late Pleistocene
G. alboguttata	NA	0.19 (0.3–0.1)	Middle/Late Pleistocene
G. argentata	NA	0.20 (0.3–0.1)	Middle/Late Pleistocene
G. egeria	0.19 (0.6–0.0)	NA	Middle/Late Pleistocene

DISCUSSION

Is *Glauconycteris* monophyletic?

The monophyly of *Glauconycteris* was supported in the molecular studies of Hoofer and Van Den Bussche (2003) and Roehrs et al. (2010, 2011) based on DNA sequences from four species of the genus. More recently, however, *Glauconycteris* appeared paraphyletic in the molecular tree of Koubínová et al. (2013), the species *G. variegata* being separated from the clade comprising *G. argentata*, *G. beatrix*, *G. egeria*, and *Arielulus cuprosus* (a species endemic to Borneo). We suspected that this result was an artefact of the high percentage of missing data in the supermatrix used in Koubínová et al. (2013): 59 % in the DNA sequences of *Glauconycteris* and 93 % in those of *A. cuprosus* (only a partial *Cytb* sequence was included in the data set). In agreement with that hypothesis, our phylogenetic analyses showed high support for the monophyly of both genera *Glauconycteris* and *Arielulus* (**Figures 4** and **5**), even when the available GenBank sequences of *A. cuprosus* were included in the *Cytb*, *12S*, and *RAG2* alignments (see results in **Figure S6**).

Only four species of *Glauconycteris* were included in previous molecular studies (Hoofer and Van Den Busschen 2003; Roehrs et al. 2010, 2011; Koubínová et al. 2013) of the 12 species that are currently recognized in the genus (Happold and Happold 2013; ACR 2016). In particular, the rarely collected species *G. superba* has not been sequenced prior to our study. In fact, Reeder et al. (2013) based their conclusion to place this species in its own genus *Niumbaha* solely on morphological characters. Our morphological analysis using both quantitative and qualitative variables (**Figure 3**) corroborates their finding that *G. superba* is readily distinguishable from other species of *Glauconycteris*, mainly based on its larger body size and unique pelage pattern. Our mtDNA and nuDNA trees (**Figures 4** and **5**) showed that *G. superba* is highly divergent

from two other lineages, i.e. *G. variegata* and a large clade uniting all other species of *Glauconycteris*. However, our nuclear analyses provided strong support for a sister-group relationship between *G. superba* and *G. variegata* (**Figure 5**), which invalidates the taxonomic conclusion of Reeder et al. (2013). Hence, we recommend that the species *G. superba* should be retained in the genus *Glauconycteris*.

On the origin and diversification of butterfly bats

Based on a mitochondrial alignment covering both 12S and 16S rRNA genes, Hoofer and Van Den Bussche (2003) concluded that the genus *Glauconycteris* belongs to the tribe Nycticeiini, which also contains *Nycticeius*, *Lasionycteris*, and the clade uniting *Eptesicus* and *Scotomanes*. Using both mitochondrial and nuclear genes, Roehrs et al. (2010, 2011) and Koubínová et al. (2013) have suggested that the tribe also includes the three Asian genera *Arielulus*, *Hesperoptenus* and *Ia*. However, none of the previous studies provided strong support for either the monophyly of the tribe Nycticeiini or the position of *Glauconycteris*.

Due to the lack of nuclear data for *Nycticeius*, our study is not really appropriate for testing the monophyly of Nycticeiini. However, it should be noted that none of our analyses supported the existence of this tribe. By contrast, all our mtDNA and nuDNA analyses (**Figure 4** and **5**) showed a strong support for a sister-group relationship between the African genus *Glauconycteris* and the Asian genus *Hesperoptenus*. In addition, these two genera share two diagnostic indels (insertion or deletion) in *HDAC2* and two others in *RIOK3* (**Figure 5**). Our nuDNA and supermatrix analyses suggest that the Asian genus *Arielulus* is the sister-group of the clade composed of *Glauconycteris* and *Hesperoptenus* (**Figure 5** and **Figure S4**). Since all species of *Arielulus* and *Hesperoptenus* are found in Southeast Asia, except *A. torquatus*, which is endemic to Taiwan (IUCN 2016), we can propose that the Asian ancestor of *Glauconycteris* originated from this region. Our molecular dating estimates suggest that the ancestor of *Glauconycteris* diverged from that of *Hesperoptenus* at around 10/11 Mya, and diversified in

Africa at around 6 Mya (**Table 1**). The ancestor of *Glauconycteris* dispersed from Asia into Africa probably during the Tortonian age of the Late Miocene (11.6-7.2 Mya), when the climate of northeastern Africa and Arabian Peninsula was less arid than today (Kürschner 1998; Pound et al. 2011).

At the end of the Miocene, around 6 ± 2 Mya, *Glauconycteris* diversified in Africa into three main groups, which today occupy different habitats: the lineage corresponding to *G. variegata* (which may also contain *G. machadoi*) is predominantly associated with savannah, woodland, and bushveld habitats (Monadjem et al. 2010; Rambaldini 2010); in the tropical rainforests, *G. superba* seems to be an open space forager, i.e. concentrating its activity above the canopy (Ing et al. 2016), whereas all other species of *Glauconycteris*, which have a smaller size and a less conspicuous colour pattern, are expected to be edge foragers, i.e. exploiting the spaces immediately below the canopy, as do the majority of bat species living in Neotropical rainforests (Tiago Marques et al. 2016). The basal diversification of *Glauconycteris* occurred when a brief event of aridity, between 6.5 and 6 Mya, was followed by more humid conditions (Bonnefille 2010). It also coincides with the first phase of diversification in the two fruit bat tribes that are endemic to Africa, i.e. Epomophorini and Scotonycterini (Nesi et al. 2013; Hassanin et al. 2015, 2016). As in *Glauconycteris*, fruit bats diversified into taxa characterized by different body sizes and different habitat types, suggesting that climatic change led to the exploitation of new ecological niches.

Our molecular dating estimates suggest that the three groups of *Glauconycteris* found in tropical rainforests, i.e. '*beatrix*', '*humeralis*', and '*poensis*', appeared during the Early Pliocene (5.3–3.6 Mya). At that time, the warmer and wetter climate led to the expansion of tropical rainforests in Africa (Bonnefille 2010; Salzmann et al. 2011), which may have offered more favourable conditions for forest-adapted bats. This was followed by the majority of speciation events during the Late Pliocene and Early Pleistocene epochs, suggesting that most of them were driven by allopatric isolation in Pleistocene forest refugia, as has previously been shown in fruit

bats of the tribe Scotonycterini (Hassanin et al. 2015). However, *Glauconycteris* species need to be sampled from additional geographic localities in Cameroon, Gabon, and West Africa, to determine the real influence of forest refugia on their evolution.

Mito-nuclear discordance for the monophyly of *G. egeria*

The species *G. egeria* is poorly represented in museum collections (Happold and Happold 2013): four from Cameroon, four from Uganda, and five from CAR, including two new specimens collected for our study. Morphologically, it can be recognized on the basis of its pelage, which is dark brown or almost black with conspicuous whitish dorsal flank-stripe, and its subquadrangular ears, which are dark brown with a conspicuous pale rim (Happold and Happold 2013; **Figure 6**). The eight individuals from southern CAR included in our molecular analyses fall into two divergent and unrelated mitochondrial haplogroups (**Figure 4**): the first haplogroup is the sister-group of *G. poensis*; whereas the second haplogroup is more closely related to *G. alboguttata*. However, the monophyly of *G. egeria* was supported in all our nuclear analyses (**Figure 5**), and by an insertion of a nucleotide A in position 559 of the *RIOK3* alignment. All these results indicate therefore that the signal provided by the mitochondrial genome is misleading.

Three non-exclusive hypotheses can be advanced to explain such a mito-nuclear discordance: different sexual dispersal behaviours, incomplete lineage sorting of ancestral mitochondrial haplotypes, and mitochondrial introgression (e.g., Ropiquet and Hassanin 2006; Nesi et al. 2011; Hassanin et al. 2013; Hassanin et al. 2015). Our analyses suggest that the southern CAR region is a key geographic area for bat species endemic to African rainforests. Indeed, divergent mitochondrial haplogroups were also detected in this region for two other forest species: *G. beatrix* (**Figure 4**) and the fruit bat species *Casinycteris argynnis* (Hassanin et al. 2015).

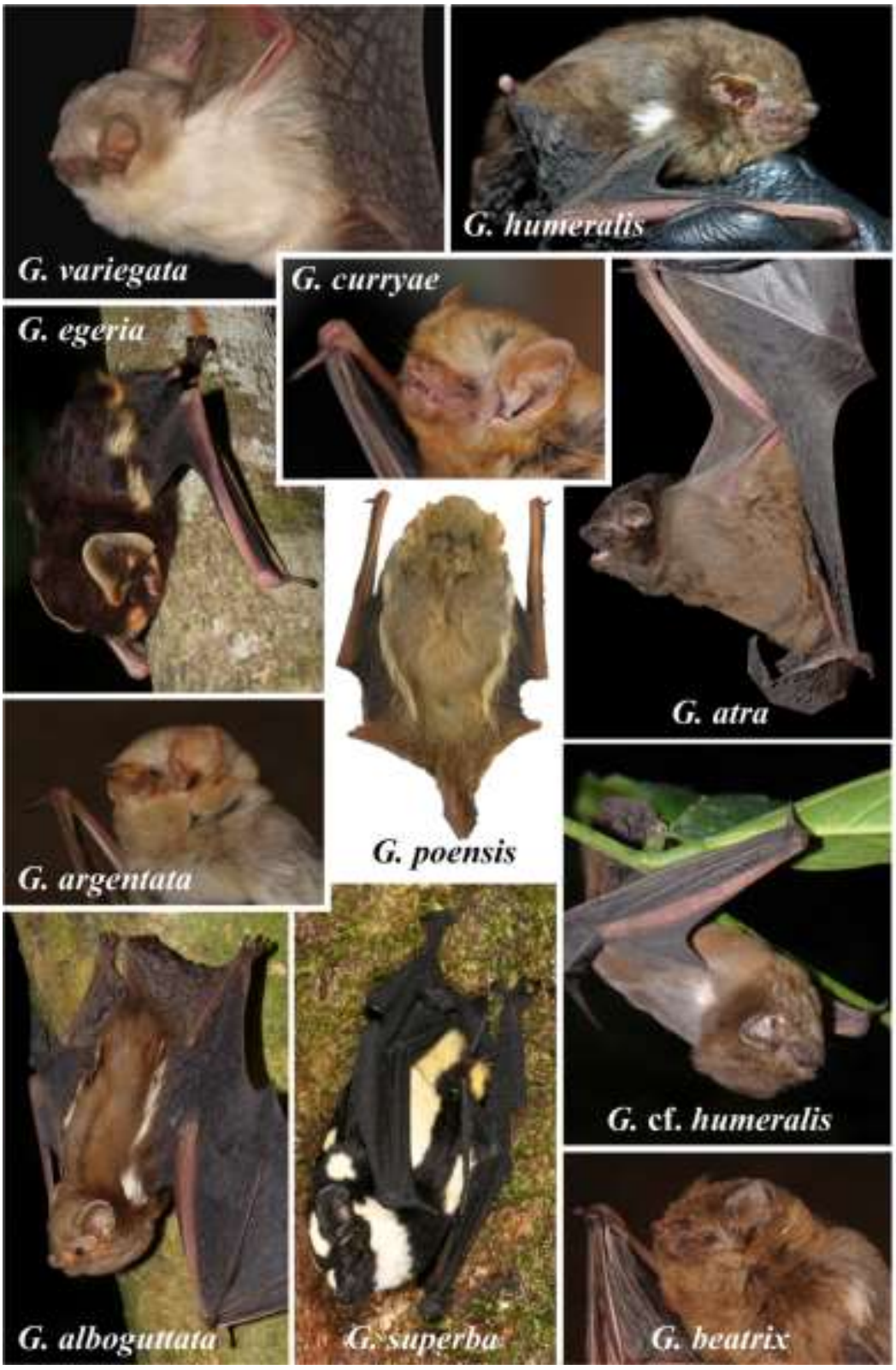

Figure 6. Colour patterns within the genus *Glauconycteris*

G. alboguttata: R13-45 (RC); *G. argentata*: MNHN 2016-2780 (AH); *G. atra* sp. nov. : MNHN 2016-2790 (RC); *G. beatrix*: MNHN 2016-2782 (AH); *G.* cf. *humeralis*: R13-46 (RC); *G. curryae*: MNHN 2016-2795 (AH); *G. egeria*: R13-21 (RC); *G. humeralis*: MNHN 2016-2802 (RC); *G. poensis*: DM 13217 (AM); *G. superba*: K13-287 (AH); *G. variegata*: ECJS-43/2009 (©Ernest Seamark).

In the two latter species, the two haplogroups represent two geographic regions: western Equatorial Africa (Gabon, Republic of the Congo, and/or southeastern Cameroon) and eastern Equatorial Africa (eastern DRC). A similar geographic division was also detected for *Scotonycteris bergmansi*, another fruit bat species endemic to the forests of Equatorial Africa (Hassanin et al. 2015). All these data suggest that southern CAR may therefore be a potential hybrid zone between bat populations isolated into distant forest refugia during glacial periods of the Pleistocene epoch, located respectively in western and eastern Equatorial Africa. In this context, female philopatry may explain the divergence of two mitochondrial haplogroups in distant western and eastern Pleistocene forest refugia, whereas male-biased dispersal may have maintained nuclear gene flow during interglacial periods. In *G. egeria*, however, it is impossible to know if the two mitochondrial haplogroups have any geographical significance, because all of our specimens were collected in CAR. Another issue that remains to be resolved is that the two mitochondrial haplogroups identified in *G. egeria* are related to two different species: the haplogroup 1 diverged from *G. poensis* at 2.2 ± 0.8 Mya, whereas the haplogroup 2 diverged from *G. alboguttata* at 1.5 ± 0.6 Mya (**Table 1**). In the absence of nuclear sequences for *G. poensis*, it is difficult to provide a reliable interpretation. However, our nuclear analyses showed that *G. egeria* is more closely related to *G. argentata* than to *G. alboguttata* (**Figure 5**). This phylogenetic result suggests that the mitochondrial genome of *G. alboguttata* was transferred into one population of *G. egeria* at around 1.5 Mya. To provide further support for this scenario, and to better understand the potential role of female philopatry and Pleistocene forest refugia, it will be necessary to sequence mitochondrial and nuclear markers from several other specimens of *G. egeria* and *G. poensis* collected in both western and eastern Equatorial Africa.

How many species exist within the '*beatrix*' and '*humeralis*' groups?

Although our molecular analyses showed that specimens identified as *G. beatrix* and *G. humeralis* belong to two distinct groups, the morphological identification of individuals to either *G. beatrix* or *G. humeralis* remains problematic (**Figure 3**).

The species *G. beatrix* was described by Thomas (1901) based on a single specimen (BMNH 1898.5.4.19) collected at the Benito River in Equatorial Guinea. As pointed out by Rosevear (1965), the description of Thomas (1901) 'was misleading as to skull length, pattern, and possibly colour'. Thomas (1901) described *G. beatrix* as 'General colour above and below uniform blackish-brown without lighter markings', but Rosevear (1965) noted that the colour of the type specimen was 'pale red brown… with white tufts on the shoulders', as described by Sanborn (1953) in several specimens from Gabon. All 16 specimens of *G. beatrix* we collected in DRC also have white shoulder-spots, and the three specimens from CAR share the same pattern. By contrast, the adult female from Cameroon (HNHM 23262) does not have white shoulder-spots. The holotype of *G. beatrix* is a female characterized by the following measurements (data from Rosevear 1965): FA=39, HB=45, TIB=19.5, 3DM=38, GLS=11.6, ZW=8.5, BCW=7.1, and MB=7.5. Our specimens identified as *G. beatrix* from Cameroon, CAR and DRC fit all these characteristics (mean values for ♀ [n=3], FA=38.5, TIB=19.7, 3DM=39.0; ♂ [n=7]: FA=36.0, TIB=18.5, 3DM=36.6; see details in **Table S2**). By contrast, the three specimens from RCI formerly identified as *G. beatrix* in the ROM collection have a smaller body size (♀ [n=1], FA=35, TIB=17.5, 3DM=34.1; ♂ [n=2]: FA=34.5, TIB=16.5, 3DM=34.6). In the mitochondrial tree (**Figure 4**), the species *G. beatrix* was found to be polyphyletic: the individuals from Central Africa constitute the sister-group of *G. curryae*, whereas the five *G. beatrix* specimens from RCI are closely related to the '*humeralis*' group. As a consequence, both morphological and molecular results suggest that the five specimens housed at the ROM (under N° 100527, 100528, 100531, 100534 and 100578) belong to a species different from *G. beatrix*, here referred to as *G.* cf. *beatrix*.

Various authors have expressed doubts about the specific status of *G. humeralis*. Koopman (1971, 1994), Peterson and Smith (1973), Eger and Schlitter (2001) and Monadjem et al. (2010) all considered it as a subspecies of *G. beatrix*. Despite their apparent morphological similarities, our molecular analyses indicate that *G. beatrix* and *G. humeralis* are not closely related. The species *G. humeralis* was described by Allen (1917) on the basis of five specimens collected in DRC: a holotype and three topotypes from Medje, and another individual from Avakubi. The measurements of the holotype (AMNH 49013, female) published by Allen (1917) are: FA=36.8, HB=42, T=40, TIB=16.8[1], 3DM=35.8, GLS=11.3, ZW=8.2, MB=7.3, C-M^3= 3.6, ML=7.9, and C-M_3=3.9. These measurements fit with those taken from a female, K13-47, that was also used in our molecular study, which was collected less than 250 km from the type locality at Medje (**Table S2**). In addition, the forearm lengths of the two female topotypes are also similar to that of K13-47 (35.8 and 35.3 *versus* 35.6 mm). By contrast, the FA is significantly larger in a female, AMNH 49014, collected at Avakubi (38.8 mm). As pointed out by Allen (1917) 'The pure white shoulder tuft is a conspicuous feature in the type and topotypes; it is present in the Avakubi specimen, but only the tips of the hairs are white (yellowish white instead of pure white)'. We therefore suggest that the Avakubi specimen (AMNH 49014) belongs instead to *G. beatrix*. This point may explain previous taxonomic confusions between *G. beatrix* and *G. humeralis*. In the DRC, we collected two species of the '*beatrix*' group, i.e. *G. beatrix* and *G. curryae*, and two species of the '*humeralis*' group, *G. humeralis* and *G. atra* sp. nov.. Whereas *G. curryae* and *G. atra* sp. nov. can be easily identified by phenotypic characteristics, such as the fur colour, *G. beatrix* and *G. humeralis* have very similar external appearances. In the light of our study, we consider, however, that three characters can be used to distinguish the two species: the shoulder spots are more conspicuous in *G. humeralis*; and FA and TIB lengths are significantly smaller in *G. humeralis* than in *G. beatrix* (**Table S2**).

[1] We assumed a typographical error, as Allen (1917) published 26.8 mm in his original description. Despite several requests to the AMNH collection managers, we did not succeed in obtaining a new measurement of the tibia length.

Within the '*humeralis*' group, our analyses suggest two potentially new species. According to our mitochondrial and nuclear analyses, the taxon identified as *G.* cf. *humeralis* may belong to a new species. Unfortunately, the individuals of *G.* cf. *humeralis*, R13-46 and R13-98, that were captured in southern CAR were released after being examined and punched for DNA sequencing. Without type specimen(s) deposited in museum collection we refrain to describe the new species herein. According to our morphological and mitochondrial analyses, the taxon here referred to as *G.* cf. *beatrix* may also be recognized as a putative new species. However, nuclear markers need to be sequenced on the five specimens housed at the ROM in order to test possible gene flow with *G. atra* sp. nov. and *G.* cf. *humeralis*.

Evolution of colour pattern within the genus *Glauconycteris*

The species of butterfly bats show a wide a variety of colours (piebald, blackish brown, dark brown, sepia brown, reddish-brown, rusty brown with yellowish tints, greyish brown, golden-fawn, creamy-fawn, and pale-brown; **Figure 6**). In addition, most species exhibit specific body patterns. Three species have reticulated wings (dark lines on pale background): *G. gleni*, *G. machadoi*, and *G. variegata*. The species *G. kenyacola* is characterized by whitish facial markings on nose and at base of ears (Happold and Happold 2013). All species of the '*poensis*' group have white or whitish stripes along the flank above the wing (*G. poensis*, *G. alboguttata*, *G. argentata*, and *G. egeria*,), suggesting that this character probably constitutes a good synapomorphy. In *G. superba*, there are two pairs of white stripes that are located more dorsally on the back. Five species have generally one spot on each shoulder: *G. alboguttata*, *G. beatrix*, *G.* cf. *beatrix*, *G.* cf. *humeralis*, and *G. humeralis*. In *G. egeria*, we observed that the shoulder-spot and dorsal flank-stripe are confluent. In *G. superba*, there are two or rarely three white spots on each shoulder (Ing et al. 2016). In addition, two species are without body patterns or reticulated wings: *G. atra* sp. nov. and *G. curryae*.

Hayman and Jones (1950) described a remarkably wide variation in the pattern of white shoulder spots and flank stripes for several individuals of *G. poensis* collected in Sierra Leone: 'Of the 40 specimens… 20 have the shoulder spots and flank stripes distinct on both sides, while six have no markings of any kind. The remaining 14 show every type of variation. Several are asymmetrical, having shoulder spots on one side only, with or without a flank stripe'. As a consequence, Hayman and Jones (1950) raised the question whether these white markings are in themselves sufficiently constant for use in specific diagnoses. In all species examined in our study, however, we found no variation in body pattern, i.e. spots and/or flank stripes are consistently present or absent in all individuals of each species. The sole exception is *G. beatrix*, in which individuals from CAR and DRC have faint white shoulder spots, whereas the individual from Cameroon does not exhibit any white markings. In addition, we never observed individuals with asymmetrical markings, i.e. with a spot on one shoulder only. More importantly, all species of the '*poensis*' group share the presence of dorsal flank-stripes. In this context, the observations published by Hayman and Jones (1950) for *G. poensis* should be regarded with caution, and all of their specimens from Sierra Leone need to be re-examined and sequenced to provide definitive conclusions on their taxonomic status and the levels of intraspecific variation in *G. poensis*.

Acknowledgements

We thank Aimée Francis Bingo, Laurent Daudet, Jean-François Julien, Emmanuel Nakouné, Nicolas Nesi, and Carine Ngoagouni for assistance with field studies. In DRC, we are very grateful to Faustin Toengaho Lokundo, the Rector of the University of Kisangani, for his invitation, and Benjamin Dudu, Hilde Keunen, Erik Verheyen, and all other members of the *Centre de Surveillance de la Biodiversité*, who provided administrative and logistic support. In CAR, we would like to acknowledge Pr. Alain Le Faou, the director of the *Institut Pasteur de Bangui*, for his invitation in 2008, and Philippe Annoyer, who organized the expedition "*Sangha 2012, Biodiversité en terre pygmée*", the Ministries of Environment and Forest, Pr. Georgette

Florence Koyt Deballé, the Rector of the University of Bangui, Dr. Bolevane Ouantinam Serge Florent and Dr. Yongo Olga.

We are very grateful to collection managers and curators who loaned museum specimens or provided measurements, pictures, or samples for DNA analyses: Leigh Richards from the DNSM; Steve Goodman and Bruce Patterson from the FMNH; and Burton Lim and Jacqueline Miller from the ROM. We also acknowledge Alexandre Hanquet and Didier Geffard-Kuriyama (UMS 2700 MNHN) for skull images, Ernest Seamark (AfricanBats) for the image of *G. variegata*, and Wilderness Safaris for supporting his fieldwork in Botswana and Zambia. AH would like to thank Meredith Happold for measurements on *Glauconycteris* species, Darina Koubínová for the Nexus file, Dos Santos Martins Carlos, Kevin Racine, and the World Bat Library (Geneva, Switzerland) for bibliography. Céline Bonillo and Stéphanie Varizat kindly helped in the laboratory work, which was supported by the MNHN, CNRS, LabEx BCDiv 2012-2013, the *Institut Langevin*, CNRS, ESPCI, Labex WIFI 2012-2013, and the ‘‘PPF *Biodiversité actuelle et fossile*’’.

REFERENCES

ACR (2016) African chiroptera report 2016. AfricanBats, Pretoria. i -xvii, 1 - 7380 pp.

Allen JA (1917) Part I. Systematic List. In: Allen, J.A., Lang H., Chapin J.P.: The American Museum Congo expedition collection of bats. *Bull. Amer. Mus. Nat. Hist*. **37:** 405-496.

Arbogast BS, Slowinski JB (1998) Pleistocene speciation and the mitochondrial DNA clock. *Science* **282:** 1955a.

Bonnefille R (2010) Cenozoic vegetation, climate changes and hominid evolution in tropical Africa. *Glob. Planet. Change* **72:** 390-411.

Bouckaert R, Heled J, Kühnert D, Vaughan T, Wu C-H, Xie D, Suchard MA, Rambaut A, Drummond AJ (2014) BEAST2: a software platform for Bayesian evolutionary analysis. *PLOS Computational Biology* **10:** e1003537.

Darriba D, Taboada GL, Doallo R, Posada D (2012) jModelTest 2: more models, new heuristics and parallel computing. *Nature Methods* **9:** 772.

Dobson GE (1875) On the genus *Chalinolobus*, with descriptions of new or little-known species. *Proc. Zool. Soc. London* **1875:** 381-388.

Edgar RC (2004) MUSCLE: multiple sequence alignment with high accuracy and high throughput. *Nucleic Acids Res*. **32:** 1792-1797.

Eger JL, Schlitter DA (2001) A new species of *Glauconycteris* from West Africa (Chiroptera: Vespertilionidae). *Acta Chiropterologica* **3:** 1-10.

Gouy M, Guindon S, Gascuel O (2010) SeaView version 4: a multiplatform graphical user interface for sequence alignment and phylogenetic tree building. *Mol. Biol. Evol*. **27:** 221-224.

Happold M, Happold D (2013) *Mammals of Africa. Volume IV: hedgehogs, shrews and bats*. Bloomsbury Publishing, London.

Hassanin A (2014) Description of a new bat species of the tribe Scotonycterini (Chiroptera, Pteropodidae) from southwestern Cameroon. *C.R. Biol*. **337:** 134-142.

Hassanin A, An J, Ropiquet A, Nguyen TT, Couloux A (2013) Combining multiple autosomal introns for studying shallow phylogeny and taxonomy of Laurasiatherian mammals: application to the tribe Bovini (Cetartiodactyla, Bovidae). *Mol. Phylogenet. Evol*. **66:** 766-775.

Hassanin A, Delsuc F, Ropiquet A, Hammer C, Jansen van Vuuren B, Matthee C, Ruiz-Garcia M, Catzeflis F, Areskoug V, Nguyen TT, Couloux A (2012) Pattern and timing of diversification of Cetartiodactyla (Mammalia, Laurasiatheria), as revealed by a comprehensive analysis of mitochondrial genomes. *C.R. Biol*. **335:** 32-50.

Hassanin A, Khouider S, Gembu G-C, Goodman SM, Kadjo B, Nesi N, Pourrut X, Nakouné E, Bonillo C (2015) The comparative phylogeography of fruit bats of the tribe Scotonycterini (Chiroptera, Pteropodidae) reveals cryptic species diversity related to African Pleistocene forest refugia. *C.R. Biol.* **338:** 197-211.

Hassanin A, Nesi N, Marin J, Kadjo B, Pourrut X, Leroy E, Gembu G-C, Musaba Akawa P, Ngoagouni C, Nakouné E, Ruedi M, Tshikung D, Pongombo Shongo C, Bonillo C (2016) Comparative phylogeography of African fruit bats (Chiroptera, Pteropodidae) provides new insights into the outbreak of Ebola virus disease in West Africa, 2014-2016. *C.R. Biol.* **339:** 517-528.

Hayman RW, Jones TS (1950) A note on pattern variation in the Vespertilionid bat *Glauconycteris poensis* (Gray). *Annals and Magazine of Natural History* **12:** 761-763.

Hill JE, Harrison DL (1987) The baculum in the Vespertilioninae (Chiroptera: Vespertilionidae) with a systematic review, a synopsis of *Pipistrellus* and *Eptesicus*, and the description of a new genus and subgenus. *Bulletin of the British Museum (Natural History): Zoology* **52:** 225-305.

Hoofer SR, Van Den Bussche RA (2003) Molecular phylogenetics of the chiropteran family Vespertilionidae. *Acta Chiropterologica* **5:** 1-63.

Ing RK, Colombo R, Gembu G-C, Bas Y, Julien J-F, Gager Y, Hassanin A (2016) Echolocation calls and flight behaviour of the elusive Pied Butterfly Bat (*Glauconycteris superba*), and new data on its morphology and ecology. *Acta Chiropterologica* **18:** 477-488.

IUCN (2016) The IUCN Red List of Threatened Species. Version 2016.2. <www.iucnredlist.org>. Downloaded on 05 September 2016.

Koopman KF (1971) Taxonomic notes on *Chalinolobus* and *Glauconycteris* (Chiroptera, Vespertilionidae). *American Museum Novitates* **2451:** 1-10.

Koopman KF (1994) Chiroptera: systematics. In: Niethammer J, Schliemann H, Starck D, eds. Handbook of Zoology. Volume 8. Berlin: Walter de Gruyter, 1-217.

Koubínová D, Irwin N, Hulva P, Koubek P, Zima J (2013) Hidden diversity in Senegalese bats and associated findings in the systematics of the family Vespertilionidae. *Front. Zool.* **10:** 48.

Kürschner H (1998) Biogeography and introduction to vegetation. In: Ghazanfar SA, Fisher M, eds. *Vegetation of the Arabian Peninsula*. Dordrecht, Kluwer Academic Publishers, 63-98.

Lack JB, Roehrs ZP, Stanley Jr CE, Ruedi M, Van Den Bussche RA (2010) Molecular phylogenetics of *Myotis* indicate familial-level divergence for the genus *Cistugo* (Chiroptera). *J. Mammal*. **91:** 976-992.

Lê S, Josse J, Husson F (2008) FactoMineR: An R Package for Multivariate Analysis. *J. Stat. Softw*. **25:** 1-18.

Meredith RW, Janečka JE, Gatesy J, Ryder OA, Fisher CA, Teeling EC, Goodbla A, Eizirik E, Simão TLL, Stadler T, Rabosky DL, Honeycutt RL, Flynn JJ, Ingram CM, Steiner C, Williams TL, Robinson TJ, Burk-Herrick A, Westerman M, Ayoub NA, Springer MS, Murphy WJ (2011) Impacts of the Cretaceous terrestrial revolution and KPg extinction on mammal diversification. *Science* **334:** 521-524.

Miller GS (1907) The families and genera of bats. *U. S. Natl. Mus. Bull.* **57:** 1-282.

Monadjem A, Richards L, Denys C (2016) An African bat hotspot: the exceptional importance of Mount Nimba for bat diversity. *Acta Chiropterologica* **18:** 359-375.

Monadjem A, Taylor P, Cotterill FPD, Schoeman MC (2010) *Bats of Southern and Central Africa: a biogeographic and taxonomic synthesis*. University of the Witwatersrand, Johannesburg, South Africa.

Nesi N, Kadjo B, Pourrut X, Leroy E, Pongombo Shongo C, Cruaud C, Hassanin A (2013) Molecular systematics and phylogeography of the tribe Myonycterini (Mammalia, Pteropodidae) inferred from mitochondrial and nuclear markers. *Mol. Phylogenet. Evol.* **66:** 126-137.

Nesi N, Nakouné E, Cruaud C, Hassanin A (2011) DNA barcoding of African fruit bats (Mammalia, Pteropodidae). The mitochondrial genome does not provide a reliable discrimination between *Epomophorus gambianus* and *Micropteropus pusillus*. *C.R. Biol.* **334:** 544-554.

Patterson BD, Webala PW (2012) Keys to the bats (Mammalia: Chiroptera) of East Africa. *Fieldiana: Life and Earth Sciences* **6:** 1-60.

Peterson RL, Smith DA (1973) A new species of *Glauconycteris* (Vespertilionidae, Chiroptera). *Life Science Occasional Papers* **22:** 1-9.

Pound MJ, Haywood AM, Salzmann U, Riding JB, Lunt DJ, Hunter SJ. (2011) A Tortonian (Late Miocene, 11.61–7.25 Ma) global vegetation reconstruction. *Paleogeogr. Paleoclimatol. Paleoecol*. **300:** 29-45.

R Core Team (2015) R: a language and environment for statistical computing. R Foundation for Statistical Computing, Vienna, Austria. URL http://www.R-project.org/.

Rambaldini DA (2010) *Glauconycteris variegata* (Chiroptera: Vespertilionidae). *Mammalian Species* **42:** 251-258.

Reeder DM, Helgen KM, Vodzak ME, Lunde DP, Ejotre I (2013) A new genus for a rare African vespertilionid bat: insights from South Sudan. *ZooKeys* **285:** 89–115.

Roehrs ZP, Lack JB, Van Den Bussche RA (2010) Tribal phylogenetic relationships within Vespertilioninae (Chiroptera: Vespertilionidae) based on mitochondrial and nuclear sequence data. *J. Mammal.* **91:** 1073-1092.

Roehrs ZP, Lack JB, Van Den Bussche RA (2011) A molecular phylogenetic reevaluation of the tribe Nycticeiini (Chiroptera: Vespertilionidae). *Acta Chiropterologica* **13:** 17-31.

Ronquist F, Teslenko M, van der Mark P, Ayres DL, Darling A, Höhna S, Larget B, Liu L, Suchard MA, Huelsenbeck JP (2012) MrBayes 3.2: efficient Bayesian phylogenetic inference and model choice across a large model space. *Syst. Biol*. **61:** 539-542.

Ropiquet A, Hassanin A (2006) Hybrid origin of the Pliocene ancestor of wild goats. *Mol. Phylogenet. Evol*. **41:** 395-404.

Ropiquet A, Li B, Hassanin A (2009) SuperTRI: a new approach based on branch support analyses of multiple independent data sets for assessing reliability of phylogenetic inferences. *C.R. Biol*. **332:** 832-847.

Rosevear DR (1965) *The bats of West Africa*. Trustees of the British Museum (Natural History), London.

Ryan RM (1966) A new and some imperfectly known Australian *Chalinolobus* and the taxonomic status of African *Glauconycteris*. *J. Mammal*. **47:** 86-91.

Salzmann U, Williams M, Haywood AM, Johnson ALA, Kender S, Zalasiewicz J (2011) Climate and environment of a Pliocene warm world. *Paleogeogr. Paleoclimatol. Paleoecol.* **309:** 1-8.

Sanborn CC (1953) Notes sur quelques mammifères de l'Afrique équatoriale française. *Mammalia* **17:** 164-169.

Swofford DL (2003) PAUP*. Phylogenetic Analysis Using Parsimony (*and Other Methods). Version 4. Sinauer Associates, Sunderland, Massachusetts.

Tate GHH (1942) Review of the vespertilionine bats, with special attention to genera and species of the Archbold collections. *Bull. Am. Mus. Nat. Hist.* **80:** 221–297.

Teeling EC, Springer MS, Madsen O, Bates P, O'Brien SJ, Murphy WJ (2005) A molecular phylogeny for bats illuminates biogeography and the fossil record. *Science* **307:** 580-584.

Thomas O (1913) On some specimens of *Glauconycteris* from the Cameroons. *Annals and Magazine of Natural History* (ser. 8) **11:** 144-145.

Thomas O (1901) New species of *Macroscelides* and *Glauconycteris*. *Annals and Magazines of Natural History* (ser. 7) **8:** 255-257.

Tiago Marques J, Ramos Pereira MJ, Palmeirim JM (2016) Patterns in the use of rainforest vertical space by Neotropical aerial insectivorous bats: all the action is up in the canopy. *Ecography* **39:** 476-486.

SUPPORTING INFORMATION

Table S1. Specimens analysed in this study

Table S2. Quantitative and qualitative variables used for morphological comparisons

Figure S1. Separate Bayesian analyses of the three mitochondrial genes

S1.1. Bayesian tree reconstructed with the alignment of 111 *CO1* sequences.

S1.2. Bayesian tree reconstructed with the alignment of 104 *Cytb* sequences.

S1.3. Bayesian tree reconstructed with the alignment of 103 *12S* sequences.

Figure S2. Separate Bayesian analyses of the five independent data sets based on 69 specimens.

S2.1. Bayesian tree reconstructed with the concatenation of the three mitochondrial genes.

S2.2. Bayesian tree reconstructed with the alignment of *HDAC2* sequences.

S2.3. Bayesian tree reconstructed with the alignment of *RAG2* sequences.

S2.4. Bayesian tree reconstructed with the alignment of *RIOK3* sequences.

S2.5. Bayesian tree reconstructed with the alignment of *ZFYVE27* sequences.

Figure S3. Sexual size dimorphism in species of *Glauconycteris*

Figure S4. Bayesian tree reconstructed with the supermatrix combining all the seven genes (6,179 characters)

Figure S5. Chronograms inferred from *RAG2* and *Cytb* alignments

S5.1. Chronogram estimated with 126 *RAG2* sequences.

S5.2. Chronogram estimated with 77 *Cytb* sequences and R1.

S5.3. Chronogram estimated with 77 *Cytb* sequences and R2.

Figure S6. Phylogenetic position of *Arielulus cuprosus* based on *Cytb, 12S* and *RAG2* alignments

S6.1. Bootstrap 50% majority-rule consensus tree obtained from the Neighbour-Joining analysis of *Cytb* sequences.

S6.2. Bootstrap 50% majority-rule consensus tree obtained from the Neighbour-Joining analysis of *12S* sequences.

S6.3. Bootstrap 50% majority-rule consensus tree obtained from the Neighbour-Joining analysis of *RAG2* sequences.

Figure S7. Map of geographic localities